Human Demographic History Impacts Genetic Risk Prediction across Diverse Populations

Alicia R. Martin,[1,2,3,4] Christopher R. Gignoux,[4] Raymond K. Walters,[1,2,3] Genevieve L. Wojcik,[4] Benjamin M. Neale,[1,2,3] Simon Gravel,[5,6] Mark J. Daly,[1,2,3] Carlos D. Bustamante,[4] and Eimear E. Kenny[7,8,9,10,*]

The vast majority of genome-wide association studies (GWASs) are performed in Europeans, and their transferability to other populations is dependent on many factors (e.g., linkage disequilibrium, allele frequencies, genetic architecture). As medical genomics studies become increasingly large and diverse, gaining insights into population history and consequently the transferability of disease risk measurement is critical. Here, we disentangle recent population history in the widely used 1000 Genomes Project reference panel, with an emphasis on populations underrepresented in medical studies. To examine the transferability of single-ancestry GWASs, we used published summary statistics to calculate polygenic risk scores for eight well-studied phenotypes. We identify directional inconsistencies in all scores; for example, height is predicted to decrease with genetic distance from Europeans, despite robust anthropological evidence that West Africans are as tall as Europeans on average. To gain deeper quantitative insights into GWAS transferability, we developed a complex trait coalescent-based simulation framework considering effects of polygenicity, causal allele frequency divergence, and heritability. As expected, correlations between true and inferred risk are typically highest in the population from which summary statistics were derived. We demonstrate that scores inferred from European GWASs are biased by genetic drift in other populations even when choosing the same causal variants and that biases in any direction are possible and unpredictable. This work cautions that summarizing findings from large-scale GWASs may have limited portability to other populations using standard approaches and highlights the need for generalized risk prediction methods and the inclusion of more diverse individuals in medical genomics.

Introduction

The majority of genome-wide association studies (GWASs) have been performed in populations of European descent.[1–4] An open question in medical genomics is the degree to which these results transfer to new populations. GWASs have yielded tens of thousands of common genetic variants significantly associated with human medical and evolutionary phenotypes, most of which have replicated in other ethnic groups.[5–7] However, GWASs are optimally powered to discover common variant associations, and the European bias in GWASs results in associated SNPs with higher minor allele frequencies on average compared to other populations. The predictive power of GWAS findings and genetic diagnostic accuracy in non-Europeans are therefore limited by population differences in allele frequencies and linkage disequilibrium structure. For example, a previous study showed that the accuracy of breeding values and genomic prediction decays approximately linearly with increasing divergence between the discovery and target population.[8] Additionally, multiple individuals with African ancestry have received false positive misdiagnoses of hypertrophic cardiomyopathy that would have been prevented with the inclusion of even small numbers of African Americans in these studies.[9] Further, a previous study finding that 96% of GWAS participants are of European descent[1] has recently been updated; although the non-European proportion of GWAS participants has increased to nearly 20%, this is primarily driven by Asian individuals, and the proportion of individuals with African and Hispanic/Latino ancestry in GWASs has remained essentially unchanged.[4]

As GWAS sample sizes grow to hundreds of thousands of samples, they also become better powered to detect rare variant associations.[10–12] Large-scale sequencing studies have demonstrated that rare variants show stronger geographic clustering than common variants.[13–15] Rare, disease-associated variants are therefore expected to track with recent population demography and/or be population restricted.[14,16–18] As the next era of GWASs expands to evaluate the disease-associated role of rare variants, it is not only scientifically imperative to include multi-ethnic populations, it is also likely that such studies will encounter increasing genetic heterogeneity in very large study populations. A comprehensive understanding of the genetic diversity and demographic history of multi-ethnic populations is critical for appropriate applications of GWASs and ultimately for ensuring that genetics does not contribute to or enhance health disparities.[4]

[1]Analytic and Translational Genetics Unit, Department of Medicine, Massachusetts General Hospital and Harvard Medical School, Boston, MA 02114, USA; [2]Program in Medical and Population Genetics, Broad Institute of Harvard and MIT, Cambridge, MA 02142, USA; [3]Stanley Center for Psychiatric Research, Broad Institute of Harvard and MIT, Cambridge, MA 02142, USA; [4]Department of Genetics, Stanford University, Stanford, CA 94305, USA; [5]Department of Human Genetics, McGill University, Montreal, QC H3A 0G1, Canada; [6]McGill University and Genome Quebec Innovation Centre, Montreal, QC H3A 0G1, Canada; [7]Department of Genetics and Genomic Sciences, Icahn School of Medicine at Mount Sinai, New York, NY 10029, USA; [8]The Charles Bronfman Institute of Personalized Medicine, Icahn School of Medicine at Mount Sinai, New York, NY 10029, USA; [9]Center of Statistical Genetics, Icahn School of Medicine at Mount Sinai, New York, NY 10029, USA; [10]Icahn Institute of Genomics and Multiscale Biology, Icahn School of Medicine at Mount Sinai, New York, NY 10029, USA
*Correspondence: eimear.kenny@mssm.edu
http://dx.doi.org/10.1016/j.ajhg.2017.03.004.

The most recent release of the 1000 Genomes Project (phase 3) provides one of the largest global reference panels of whole-genome sequencing data, enabling a broad survey of human genetic variation.[19] The depth and breadth of diversity queried facilitates a deep understanding of the evolutionary forces (e.g., selection and drift) shaping existing genetic variation in present-day populations that contribute to adaptation and disease.[20–25] Studies of admixed populations have been particularly fruitful in identifying genetic adaptations and risk for diseases that are stratified across diverged ancestral origins.[26–31] Admixture patterns became especially complex during the peopling of the Americas, with extensive recent admixture spanning multiple continents. Processes shaping structure in these admixed populations include sex-biased migration and admixture, isolation-by-distance, differential drift in mainland versus island populations, and variable admixture timing.[14,32,33]

Standard GWAS strategies approach population structure as a nuisance factor. A typical stepwise procedure first detects dimensions of global population structure in each individual, using principal-component analysis (PCA) or other methods,[34–37] and often excludes "outlier" individuals from the analysis and/or corrects for inflation arising from population structure in the statistical model for association. Such strategies reduce false positives in test statistics, but can also reduce power for association in heterogeneous populations and are less likely to work for rare variant association.[38,39] Recent methodological advances have leveraged patterns of global and local ancestry for improved association power,[27,40,41] fine-mapping,[42] and genome assembly.[43] At the same time, population genetic studies have demonstrated the presence of fine-scale sub-continental structure in the African, Native American, and European components of populations from the Americas.[44–47] If trait-associated variants follow the same patterns of demography, then we expect that modeling sub-continental ancestry may enable their improved detection in admixed populations.

The dawn of the GWAS era saw limited success in identifying genome-wide significant loci associated with disease, and a major endeavor to better understand the genetic architecture of complex traits emerged. The peaks that met genome-wide significance typically did not explain a significant fraction of the phenotypic variance, and a major goal to estimate how many more signals remained yet to be discovered arose; this objective ushered in a wave of methodological development in heritability, linear mixed models, and polygenic risk prediction, as discussed and reviewed extensively elsewhere.[11,48–56] Numerous complex traits have been studied with cohort sizes in the hundreds of thousands, and yet in each case there are many more signals that improve prediction accuracy than meet genome-wide significance.[48,57–59] For example, including only genome-wide significant loci in the prediction of schizophrenia explains <3% of the phenotypic variance, whereas loci meeting the significance threshold that optimally balances signal versus noise (in this case, $p \leq 0.1$) in the meta-analysis explains considerably more (>18%) of the phenotypic variance.[11] Because the prediction accuracy, which is usually measured via prediction R^2, Nagelkerke's R^2, or receiver operator curve AUC, of polygenic risk scores is currently low for most traits,[56] genetic risk prediction is not clinically viable at present, but polygenic risk scores have nonetheless repeatedly proven valuable in research contexts across a multitude of complex traits[11,48,60–65] and will become increasingly useful as GWAS sample sizes grow.[59] Additionally, several methodological advancements to the standard approach have recently been undertaken.[58,66–68]

In this study, we explore the impact of population diversity on the landscape of variation underlying human traits. We infer demographic history for the global populations in the 1000 Genomes Project, focusing particularly on admixed populations from the Americas, which are underrepresented in medical genetic studies.[4] We disentangle local ancestry to infer the ancestral origins of these populations. We link this work to ongoing efforts to improve study design and disease variant discovery by quantifying biases in clinical databases and GWASs in diverse and admixed populations. These biases have a striking impact on genetic risk prediction; for example, a previous study calculated polygenic risk scores for schizophrenia in East Asians and Africans based on GWAS summary statistics derived from a European cohort and found that prediction accuracy was reduced by more than 50% in non-European populations.[67] To disentangle the role of demography on polygenic risk prediction derived from single-ancestry GWASs, we designed a coalescent-based simulation framework reflecting modern human population history and show that polygenic risk scores derived from European GWASs are biased when applied to diverged populations. Specifically, we identify reduced variance in risk prediction with increasing divergence from Europe reflecting decreased overall variance explained, and demonstrate that an enrichment of low-frequency risk and high-frequency protective alleles contribute to an overall protective shift in European inferred risk on average across traits. Our results highlight the need for the inclusion of more diverse populations in GWASs as well as genetic risk prediction methods improving transferability across populations.

Material and Methods

Ancestry Deconvolution

We used the phased haplotypes from the 1000 Genomes consortium. We phased reference haplotypes from 43 Native American samples from Mao et al.[69] inferred to have >0.99 Native ancestry in ADMIXTURE using SHAPEIT2 (v.2.r778),[70] then merged the haplotypes using scripts made publicly available. These combined phased haplotypes were used as input to the PopPhased version of RFMix v.1.5.4[71] with the following flags: -w 0.2, -e 1, -n 5, --use-reference-panels-in-EM, --forward-backward EM. The node size of 5 was selected to reduce bias in

random forests resulting from unbalanced reference panel sizes (AFR panel N = 504, EUR panel N = 503, and NAT panel N = 43). We used the default minimum window size of 0.2 cM to enable model comparisons with previously inferred models using *Tracts*.[72] We used 1 EM iteration to improve the local ancestry calls without substantially increasing computational complexity. We used the reference panel in the EM to take better advantage of the Native American ancestry tracts from the Hispanic/Latinos in the EM given the small NAT reference panel. We set the LWK, MSL, GWD, YRI, and ESN as reference African populations, the CEU, GBR, FIN, IBS, and TSI as reference European populations, and the samples from Mao et al.[69] with inferred >0.99 Native ancestry as reference Native American populations, as in Abecasis et al.[73]

Ancestry-Specific PCA

We performed ancestry-specific PCA, as described in Moreno-Estrada et al.[32] The resulting matrix is not necessarily orthogonalized, so we subsequently performed singular value decomposition in python 2.7 using numpy. There were a small number of major outliers, as seen previously.[32] There was one outlier (ASW individual NA20314) when analyzing the African tracts, which was expected as this individual has no African ancestry. There were eight outliers (PUR HG00731, PUR HG00732, ACB HG01880, ACB HG01882, PEL HG01944, ACB HG02497, ASW NA20320, ASW NA20321) when analyzing the European tracts. Some of these individuals had minimal European ancestry, had South or East Asian ancestry misclassified as European ancestry resulting from a limited 3-way ancestry reference panel, or were unexpected outliers. As described in the PCAmask manual, a handful of major outliers sometimes occur. As AS-PCA is an iterative procedure, we therefore removed the major outliers for each sub-continental analysis and orthogonalized the matrix on this subset.

Tracts

The RFMix output was collapsed into haploid bed files, and "UNK" or unknown ancestry was assigned where the posterior probability of a given ancestry was <0.90. These collapsed haploid tracts were used to infer admixture timings, quantities, and proportions for the ACB and PEL (new to phase 3) using *Tracts*.[72] Because the ACB have a very small proportion of Native American ancestry, we fit three 2-way models of admixture, including one model of single- and two models of double-pulse admixture events, using *Tracts*. In both of the double-pulse admixture models, the model includes an early mixture of African and European ancestry followed by another later pulse of either European or African ancestry. We randomized starting parameters and fit each model 100 times and compared the log-likelihoods of the model fits. The single-pulse and double-pulse model with a second wave of African admixture provided the best fits and reached similar log-likelihoods, with the latter showing a slight improvement in fit.

We next assessed the fit of nine different models in *Tracts* for the PEL,[72] including several two-pulse and three-pulse models. Ordering the populations as NAT, EUR, and AFR, we tested the following models: ppp_ppp, ppp_pxp, ppp_xxp, ppx_xxp, ppx_xxp_ppx, ppx_xxp_pxx, ppx_xxp_pxp, ppx_xxp_xpx, and ppx_xxp_xxp, where the order of each letter corresponds with the order of populations given above, an underscore indicates a distinct migration event with the first event corresponding with the most generations before present, p corresponds with a pulse of the ordered ancestries, and x corresponds with no input from the ordered ancestries. We tested all nine models preliminarily three times, and for all models that converged and were within the top three models, we subsequently fit each model with 100 starting parameter randomizations.

Imputation Accuracy

Imputation accuracy was calculated using a leave-one-out internal validation approach. Two array designs were compared for this analysis: Illumina OmniExpress and Affymetrix Axiom World Array LAT. Sites from these array designs were subset from chromosome 9 of the 1000 Genomes Project Phase 3 release for admixed populations. After fixing these sites, each individual was imputed using the rest of the dataset as a reference panel.

Overall imputation accuracy was binned by minor allele frequency (0.5%–1%, 1%–2%, 2%–3%, 3%–4%, 4%–5%, 5%–10%, 10%–20%, 20%–30%, 30%–40%, 40%–50%) comparing the genotyped true alleles to the imputed dosages. A second round of analyses stratified the imputation by local ancestry diplotype, which was estimated as described earlier. Within each ancestral diplotype (AFR_AFR, AFR_NAT, AFR_EUR, EUR_EUR, EUR_NAT, NAT_NAT), imputation accuracy was again estimated within MAF bins.

Empirical Polygenic Risk Score Inferences

In the most standard approach, genetic risk scores for a target cohort are generated using genome-wide summary statistics from a discovery GWAS with a set of SNPs common to both studies. From this starting set of SNPs, a further reduced set of pruned, approximately independent SNPs are then identified through a greedy clumping algorithm. Typically, progressively larger sets of SNPs defined by a range of p value thresholds (e.g., $p < 5 \times 10^{-8}$, 1×10^{-5}, 1×10^{-4}, 1×10^{-3}, 0.01, etc.) are evaluated to identify the best model balancing the signal to noise ratio to maximize phenotypic variance explained.[57,58] Once the optimal significance threshold and the final set of pruned, approximately independent set of SNPs have been selected, a polygenic risk score for each individual in a target sample is computed as the sum of the count of risk alleles weighted by the effect size (e.g., log odds ratio).

To compute polygenic risk scores in the 1000 Genomes samples using summary statistics from previous GWASs, we first filtered to biallelic SNPs and removed ambiguous AT/GC SNPs from the integrated 1000 Genome call set. To get relatively independent associations when multiple significant p value associations are in the same region in a GWAS (i.e., in LD), we performed clumping in plink using the --clump flag for all variants with MAF $\geq$ 0.01,[74] which uses a greedy algorithm ordering SNPs by p value, then selectively removes SNPs within close proximity and LD in ascending p value order (i.e., starting with the most significant SNP). As a population cohort with similar LD patterns to the study sets, we used European 1000 Genomes samples (CEU, GBR, FIN, IBS, and TSI). To compute the polygenic risk scores, we considered all SNPs with p values $\leq 1 \times 10^{-2}$ in the GWAS, a window size of 250 kb, and an R^2 threshold of 0.5 in Europeans to group SNPs. After obtaining the most significant, approximately independent signals (Table S4), we computed polygenic scores using the --score flag in plink.[74]

Polygenic Risk Score Simulations

We simulated genotypes in a coalescent framework with msprime v.1.3[75] for chromosome 20 incorporating a recombination map of GRCh37 and an assumed mutation rate of 2×10^{-8} mutations / (base pair * generation). We used a demographic model previously

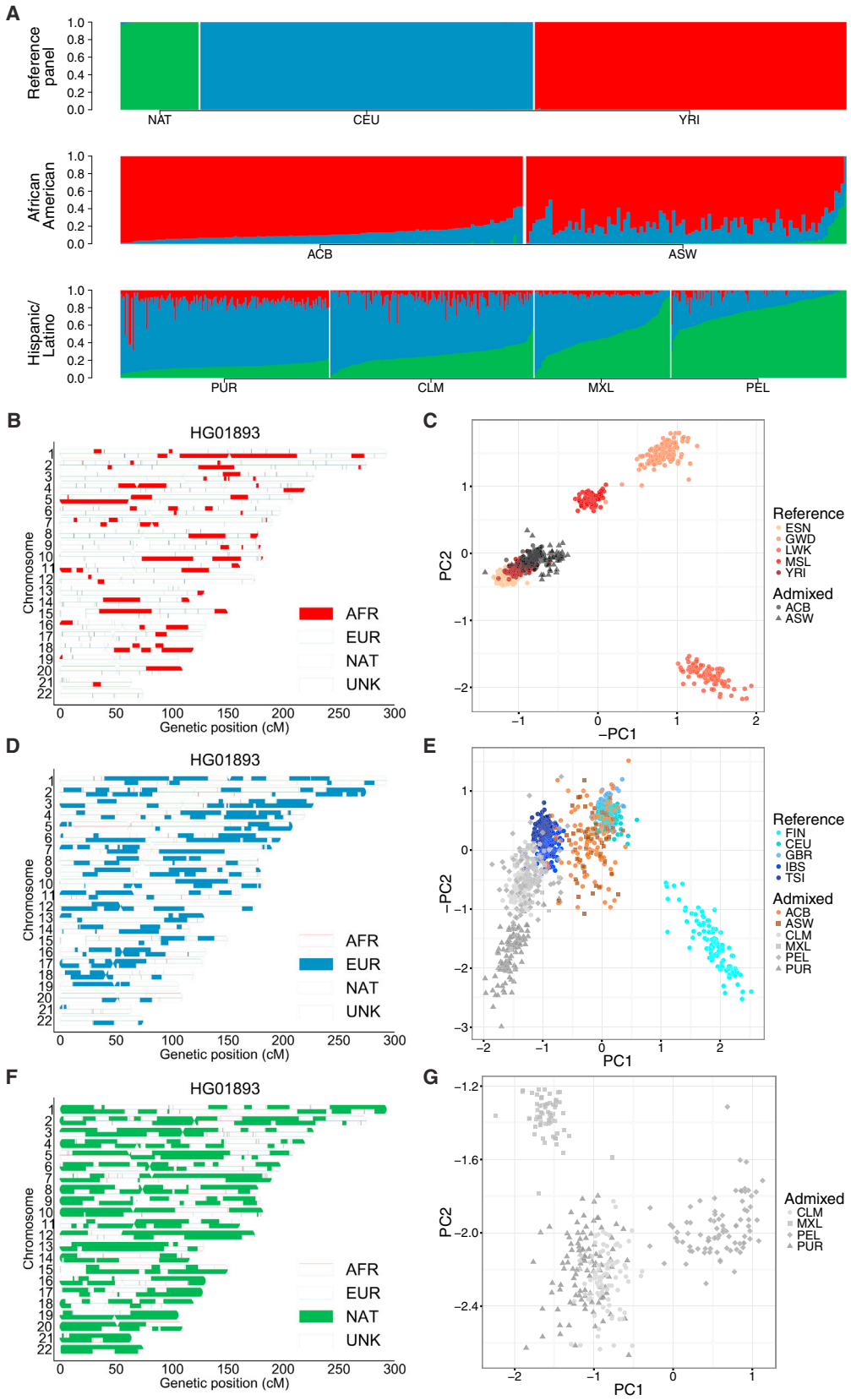

Figure 1. Sub-continental Diversity and Origins of African, European, and Native American Components of Recently Admixed American Populations

(A) ADMIXTURE analysis at K = 3 focusing on admixed Americas samples, with the NAT,[69] CEU, and YRI as reference populations.

(legend continued on next page)

inferred using 1000 Genomes sequencing data[14] to simulate individuals that reflect European, East Asian, and African population histories. We focus on these populations as the demography has previously been modeled and this avoids the challenges of simulating the geographically heterogeneous[47] and sex-biased process of admixture in the Americas.[76] To imitate a GWAS with European sample bias and evaluate polygenic risk scores in other populations, we simulated 200,000 European, 200,000 East Asian, and 200,000 African individuals. Next, we assigned "true" causal effect sizes to m evenly spaced alleles. Specifically, we randomly assigned effect sizes as

$$\beta \sim N\left(0, \frac{h^2}{m}\right)$$

where the normal distribution is specified by the mean and standard deviation (as in python's numpy package). For all other non-causal sites, the effect size is zero. We then define X as

$$X = \sum_{i=1}^{m} g_i \beta_i$$

where g_i are the genotype states (i.e., 0, 1, or 2). To handle varying allele frequencies and potential weak LD between causal sites, to ensure a neutral model with random true polygenic risks with respect to allele frequencies, and to obtain the total desired variance, we normalize X as

$$Z_X = \frac{X - \mu_X}{\sigma_X}.$$

We then compute the true polygenic risk score as

$$G = \sqrt{h^2} * Z_X$$

such that the total variance of the scores is h^2. We also simulated environmental noise and standardize to ensure equal variance between normalized genetic and environmental effects before, defining the environmental effect E as

$$\varepsilon = N(0, 1 - h^2)$$

$$Z_\varepsilon = \frac{\varepsilon - \mu_\varepsilon}{\sigma_\varepsilon}$$

$$E = \sqrt{1 - h^2} * Z_\varepsilon$$

such that the total variance of the environmental effect is $1 - h^2$. We then define the total liability as

$$L = \sqrt{h^2} * Z_X + \sqrt{1 - h^2} * Z_\varepsilon$$

$$= G + E.$$

We assigned 10,000 European individuals at the most extreme end of the liability threshold "case" status assuming a prevalence of 5%. We randomly assigned 10,000 different European individuals "control" status. We ran a GWAS with these 10,000 European case subjects and 10,000 European control subjects, computing Fisher's exact test for all sites with MAF > 0.01. As before for empirical polygenic risk score calculations from real GWAS summary statistics, we clumped these SNPs into LD blocks for all sites with $p \leq 1 \times 10^{-2}$, and $R^2 \leq 0.5$ in Europeans within a window size of 250 kb. We used these SNPs to compute inferred polygenic risk scores as before, summing the product of the log odds ratio and genotype for the true polygenic risk in a cohort of 10,000 simulated European, African, and East Asian individuals (all not included in the simulated GWAS). We compared the true versus inferred polygenic risk scores for these individuals across varying complexities (m = 200, 500, 1,000) and heritabilites (h^2 = 0.33, 0.50, 0.67).

Results

Genetic Diversity within and between Populations in the Americas

We first assessed the overall diversity at the global and sub-continental level of the 1000 Genomes Project (phase 3) populations[19] using a likelihood model via ADMIXTURE[77] and PCA[78] (Figures S1 and S2). The six populations from the Americas demonstrate considerable continental admixture, with genetic ancestry primarily from Europe, Africa, and the Americas, recapitulating previously observed population structure.[19] To quantify continental genetic diversity in these populations, we repeated the analysis using YRI, CEU, and NAT[69] samples as reference panels (population labels and abbreviations in Table S1). We observed widely varying continental admixture contributions in the six populations from the Americas at K = 3 (Figure 1A and Table S2). For example, when compared to the ASW, the ACB have a higher proportion of African ancestry ($\mu = 0.88$, 95% CI = [0.87–0.89] versus $\mu = 0.76$, 95% CI = [0.73–0.78]; two-sided t test $p = 3.0 \times 10^{-13}$) and a smaller proportion of EUR and NAT ancestry. The PEL have more NAT ancestry than all of the other AMR populations ($\mu = 0.77$, 95% CI = [0.75–0.80] versus CLM: $\mu = 0.26$, 95% CI = [0.24, 0.27], $p = 2.9 \times 10^{-95}$; PUR: $\mu = 0.13$, 95% CI = [0.12, 0.13], $p = 4.8 \times 10^{-93}$; and MXL: $\mu = 0.47$, 95% CI = [0.43, 0.50], $p = 1.7 \times 10^{-28}$) ascertained in 1000 Genomes.

We explored the origin of the subcontinental-level ancestry from recently admixed individuals by identifying local ancestry tracts[26,32,71,79] (Material and Methods, Figure S3). As proxy sources of populations for the recent admixture, we used EUR and AFR continental samples from the 1000 Genomes Project as well as NAT samples genotyped previously.[69] Concordance between global ancestry estimates inferred using ADMIXTURE at K = 5 and RFMix was typically high (Pearson's correlation ≥98%, see Figure S4). Using *Tracts*,[72] we modeled

(B, D, and F) Local ancestry karyograms for representative PEL individual HG01893 with (B) African, (D) European, and (F) Native American components shown.
(C, E, and G) Ancestry-specific PCA applied to admixed haploid genomes as well as ancestrally homogeneous continental reference populations from 1000 Genomes (where possible) for (C) African tracts, (E) European tracts, and (G) Native American tracts. A small number of admixed samples that constituted major outliers from the ancestry-specific PCA analysis were removed, including (C) one ASW sample (NA20314) and (E) eight samples, including three ACB, two ASW, one PEL, and two PUR samples.

the length distribution of the AFR, EUR, and NAT tracts to infer that admixing began ~12 and ~8 generations ago in the PEL and ACB populations, respectively (Figure S5), consistent with previous estimates from other populations from the Americas.[44,72,32]

We further investigated the subcontinental ancestry of admixed populations from the Americas one ancestry at a time using a version of PCA modified to handle highly masked data (ancestry-specific or AS-PCA) as implemented in PCAmask.[32] Example ancestry tracts in a PEL individual subset to AFR, EUR, and NAT components are shown in Figures 1B, 1D, and 1F, respectively. Consistent with previous observations, the inferred European tracts in Hispanic/Latino populations most closely resemble southern European IBS and TSI populations with some additional drift[32] (Figure 1E). The European tracts of the PUR are more differentiated compared to the CLM, MXL, and PEL populations, consistent with sex bias (Figure S6 and Table S3) and excess drift from founder effects in this island population.[32] In contrast to the southern European tracts from the Hispanic/Latino populations, the African descent populations in the Americas have European admixture that more closely resembles the northwestern CEU and GBR European populations. The clusters are less distinct, owing to lower overall fractions of European ancestry, but the European components of the Hispanic/Latino and African American populations are significantly different (Wilcoxon rank sum test $p = 2.4 \times 10^{-60}$).

The ability to localize aggregated ancestral genomic tracts enables insights into the evolutionary origins of admixed populations. To disentangle whether the considerable Native American ancestry in the ASW individuals arose from recent admixture with Hispanic/Latino individuals or recent admixture with indigenous Native American populations, we queried the European tracts. We find that the European tracts of all ASW individuals with considerable Native American ancestry are well within the ASW cluster and project closer in Euclidean distance with AS-PC1 and AS-PC2 to northwestern Europe than the European tracts from Hispanic/Latino samples ($p = 1.15 \times 10^{-3}$), providing support for the latter hypothesis and providing regional nuance to previous findings.[44]

We also investigated the African origin of the admixed AFR/AMR populations (ACB and ASW), as well as the Native American origin of the Hispanic/Latino populations (CLM, MXL, PEL, and PUR). The African tracts of ancestry from the AFR/AMR populations project closer to the YRI and ESN of Nigeria than the GWD, MSL, and LWK populations (Figure 1C). This is consistent with slave records and previous genome-wide analyses of African Americans indicating that most sharing occurred in West and West-Central Africa.[80–82] There are subtle differences between the African origins of the ACB and ASW populations (e.g., difference in distance from YRI on AS-PC1 and AS-PC2 $p = 6.4 \times 10^{-6}$), likely due either to mild island founder effects in the ACB samples or differences in African source populations for enslaved Africans who remained in Barbados versus those who were brought to the USA. The Native tracts of ancestry from the AMR populations first separate the southernmost PEL populations from the CLM, MXL, and PUR on AS-PC1, then separate the northernmost MXL from the CLM and PUR on AS-PC2, consistent with a north-south cline of divergence among indigenous Native American ancestry (Figure 1G).[32,83]

Impact of Continental and Sub-continental Diversity on Disease Variant Mapping

To investigate the role of ancestry in phenotype interpretation from genetic data, we assessed diversity across populations and local ancestries for recently admixed populations across the whole genome and sites from two reference databases: the GWAS catalog and ClinVar pathogenic and likely pathogenic sites. We recapitulate results showing that there is less variation across the genome (both genome-wide and on the Affymetrix 6.0 GWAS array sites used in local ancestry calling) in out-of-Africa versus African populations, but that GWAS variants are more polymorphic in European and Hispanic/Latino populations (Figures S7A, S7B, S8A, and S8B). We use a normalized measure of the minor allele frequency, an indicator of the amount of diversity captured in a population, to obtain a background coverage of each population, as done previously (e.g., Figure S4 from Auton et al.[19]). We show that the Affymetrix 6.0 array has a slight European bias (Figures S5A and S6A). We compared the site frequency spectrum of variants across the genome versus at GWAS catalog sites and identify elevated allele frequencies at GWAS catalog loci, particularly in populations with more European ancestry (e.g., the EUR, AMR, and SAS super populations, Figures S5C and S5D). We further compared heterozygosity (estimated here as $2pq$) and the site frequency spectrum in recently admixed populations across diploid and haploid local ancestry tracts, respectively. Sites in the GWAS catalog and ClinVar are more and less common than genome-wide variants, respectively (Figure 2). Whereas heterozygosity across the whole genome is highest in African ancestry tracts, it is consistently the greatest in European ancestry tracts across these databases (Figures 2, S8C, and S8D), reflecting a strong bias toward European study participants.[1–4,19,84] These results highlight imbalances in genome interpretability across local ancestry tracts in recently admixed populations and the utility of analyzing these variants jointly with these ancestry tracts over genome-wide ancestry estimates alone.

We also assessed imputation accuracy across the 3-way admixed populations from the Americas (CLM, MXL, PEL, PUR) for two arrays: the Illumina OmniExpress and the Affymetrix Axiom World Array LAT. Imputation accuracy was estimated as the correlation (r^2) between the original genotypes and the imputed dosages. For both array designs, imputation accuracy across all minor allele frequency (MAF) bins was highest for populations with the largest proportion of European ancestry (PUR) and

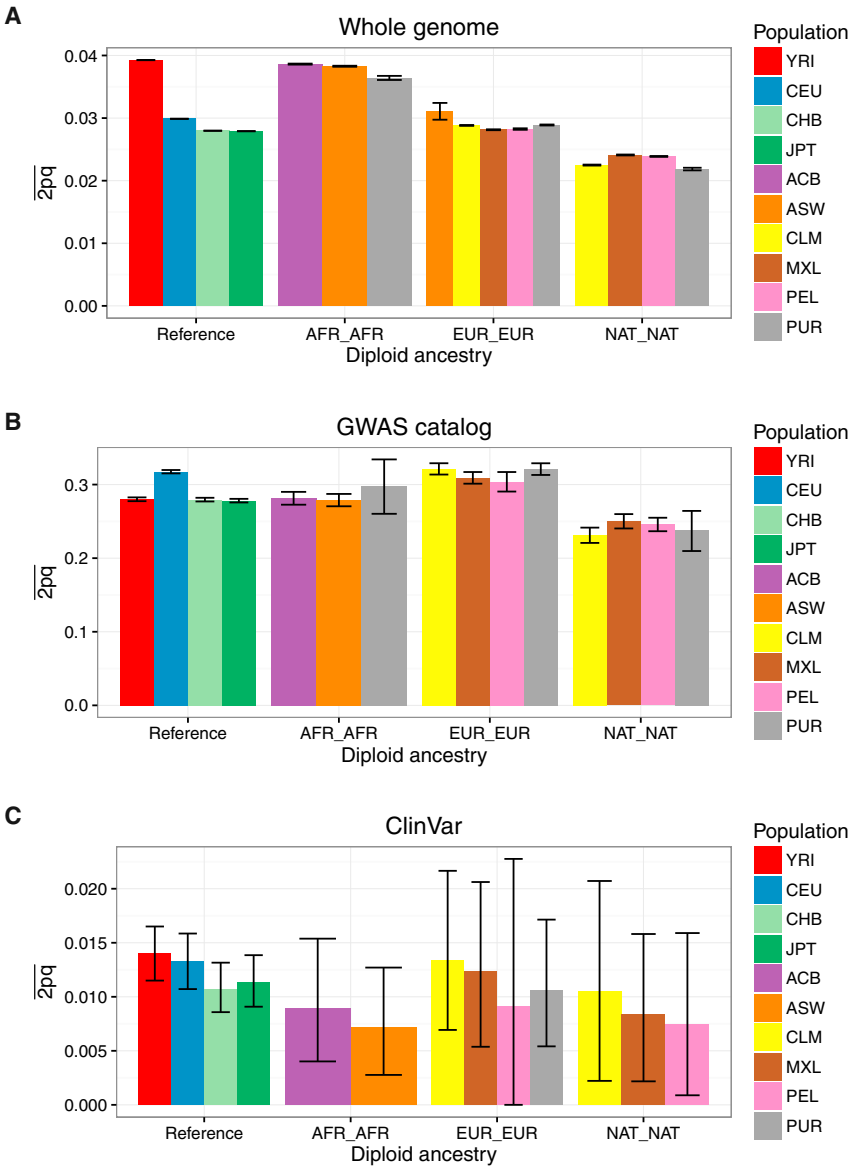

Figure 2. Heterozygosity by Continental and Diploid Local Ancestry

Heterozygosity, estimated here as 2pq, is calculated in admixed populations stratified by diploid local ancestry in (A) the whole genome, (B) sites from the GWAS catalog, and (C) sites from ClinVar classified as "pathogenic" or "likely pathogenic." The mean and 95% confidence intervals were calculated by bootstrapping 1,000 times. Populations not shown in a given panel have too few diploid ancestry tracts overlapping sites to calculate heterozygosity.

lowest for populations with the largest proportion of Native American ancestry (PEL, Figures S9A and S9B). We also stratified imputation accuracy by local ancestry tract diplotype within the Americas. Consistently, tracts with at least one Native American ancestry tract had lower imputation accuracy when compared to tracts with only European and/or African ancestry (Figures 3 and S10).

Transferability of GWAS Findings across Populations

To quantify the transferability of European-biased genetic studies to other populations, we next used published GWAS summary statistics to infer polygenic risk scores[48] across populations for well-studied traits, including height,[10] waist-hip ratio,[85] schizophrenia,[11] type II diabetes,[86,87] and asthma[88] (Figures 4A–4D and S11, Material and Methods). Most of these summary statistics are derived from studies with primarily European cohorts, although GWASs of type II diabetes have been performed in both European-specific cohorts as well as across multi-ethnic cohorts. We identify clear directional inconsistencies in these inferred scores. For example, although the height summary statistics show the expected southern/northern cline of increasing European height (FIN, CEU, and GBR populations have significantly higher polygenic risk scores than IBS and TSI, $p = 1.5 \times 10^{-75}$, Figure S9A), polygenic scores for height across super populations show biased predictions; the African populations sampled are genetically predicted to be considerably shorter than all Europeans and minimally taller than East Asians (Figure 4A), which contradicts empirical observations (with the exception of some indigenous pygmy/pygmoid populations).[89,90] Additionally, polygenic risk scores for schizophrenia, while at a similar prevalence across populations where it has been well studied[91] and sharing significant genetic risk across populations,[92] shows considerably decreased scores in Africans compared to all other populations (Figure 4B). Lastly, the relative order of polygenic risk scores computed for type II diabetes across populations differs depending on whether the summary statistics are derived from a European-specific (Figure 4C) or multi-ethnic (Figure 4D) cohort.

Ancestry-Specific Biases in Polygenic Risk Score Estimates

We performed coalescent simulations to determine how GWAS signals discovered in one ancestral case/control cohort (i.e., "single-ancestry" GWAS) are expected to impact polygenic risk score estimates in other populations under neutrality using summary statistics (for details, see Material and Methods). In brief, we simulated variants according to a previously published demographic model inferred from Africans, East Asians, and Europeans.[14] We

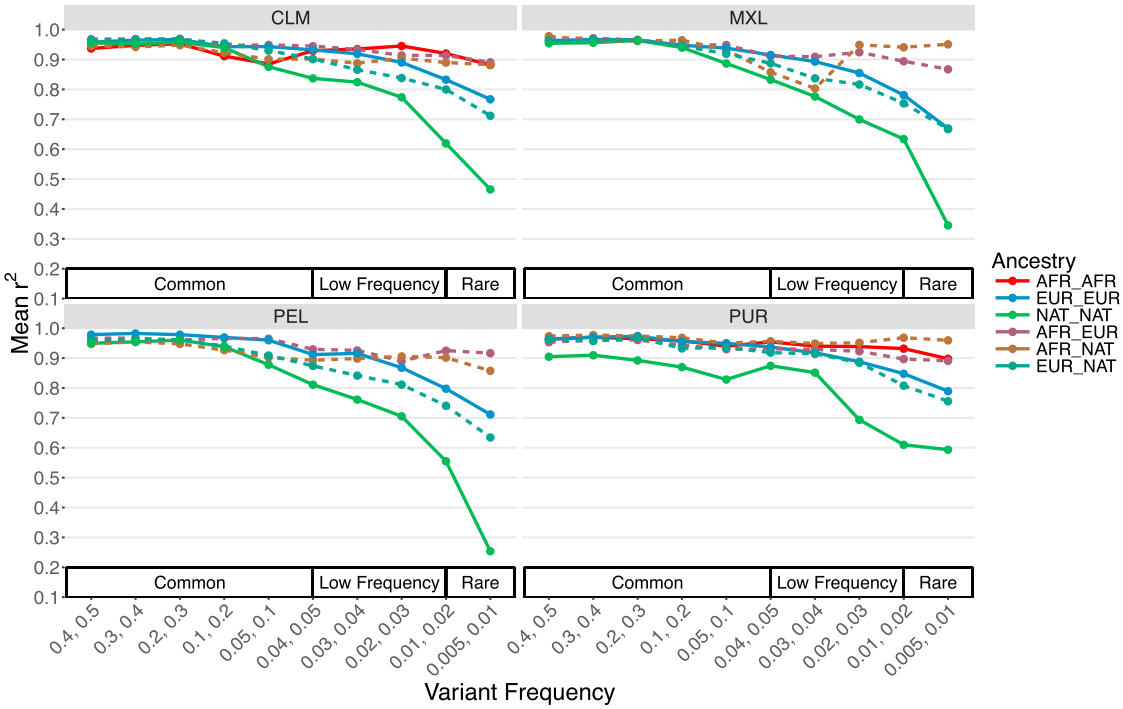

Figure 3. Imputation Accuracy by Local Ancestry in the Americas
Accuracy was assessed via a leave-one-out strategy, stratified by diploid local ancestry on chromosome 9 for the Illumina OmniExpress genotyping array. Dashed lines indicate heterozygous diploid ancestry, and solid lines show homozygous diploid ancestry.

specified "causal" alleles and effect sizes randomly, such that each causal variant has evolved neutrally and has a mean effect of zero with the standard deviation equal to the global heritability divided by number of causal variants. We computed the true polygenic risk for each individual as the product of the estimated effect sizes and genotypes, then standardized the scores across all individuals. We calculated the total liability as the sum of the genetic and random environmental contributions, then identified 10,000 European case subjects with the most extreme liabilities and 10,000 other European control subjects. We computed Fisher's exact tests with this European case-control cohort, then quantified inferred polygenic risk scores as the sum of the product of genotypes and log odds ratios for 10,000 samples per population not included in the GWAS.

In our simulations and consistent with realistic coalescent models, most variants are rare and population specific; "causal" variants are sampled from the global site frequency spectrum, resulting in subtle differences in true polygenic risk across populations (Figures S12, 5A, and 5B). We mirrored standard practices for performing a GWAS and computing polygenic risk scores (see above and Material and Methods). While causal variants in our simulations are drawn from the global site frequency spectrum and are therefore mostly rare, inferred scores are derived specifically from common variants that are typically much more common in the study population than elsewhere (here Europeans with case/control MAF $\geq$ 0.01). Consequently, while the distribution of mean true polygenic risk across simulation runs for each population are not significantly different (Figure 5A), the inferred risk is less than zero in Europeans ($p = 1.9 \times 10^{-54}$, 95% CI = [−84.3, −67.4]), slightly less than zero in East Asians ($p = 5.9 \times 10^{-5}$, 95% CI = [−19.1, −6.6]), and not significantly different from zero in Africans (Figure 5B); the variance in inferred risk scores, a proxy for the fraction of heritable variation explained, also decreases with this trend. Specifically, when $h^2 = 0.67$ and $m = 1{,}000$ causal markers, we find that the true and inferred polygenic risk scores in the EUR population are significantly correlated (i.e., non-zero, mean $\rho = 0.59$, $p < 1 \times 10^{-200}$), but the correlations in EAS and AFR populations are significantly less than in EUR ($\rho = 0.35$ and $p = 1.5 \times 10^{-48}$, $\rho = 0.22$ and $p < 1 \times 10^{-200}$, respectively). Because of allele frequency differences, number of SNPs, and inferred effect size differences along the frequency spectrum, the scale is orders of magnitude different between the true and inferred raw, unstandardized scores, cautioning that while they are informative on a relative scale (Figures 5C and S11), their absolute scale should not be over interpreted. The inferred risk difference between populations is driven by the increased power to detect minor risk alleles rather than protective alleles in the study population,[93] given the differential selection of case and control subjects in the liability threshold model. We demonstrate this empirically in these neutral simulations within the European population (Figure S14A), indicating that this phenomenon occurs even in the absence of population structure and when case and control cohort sizes are equal.

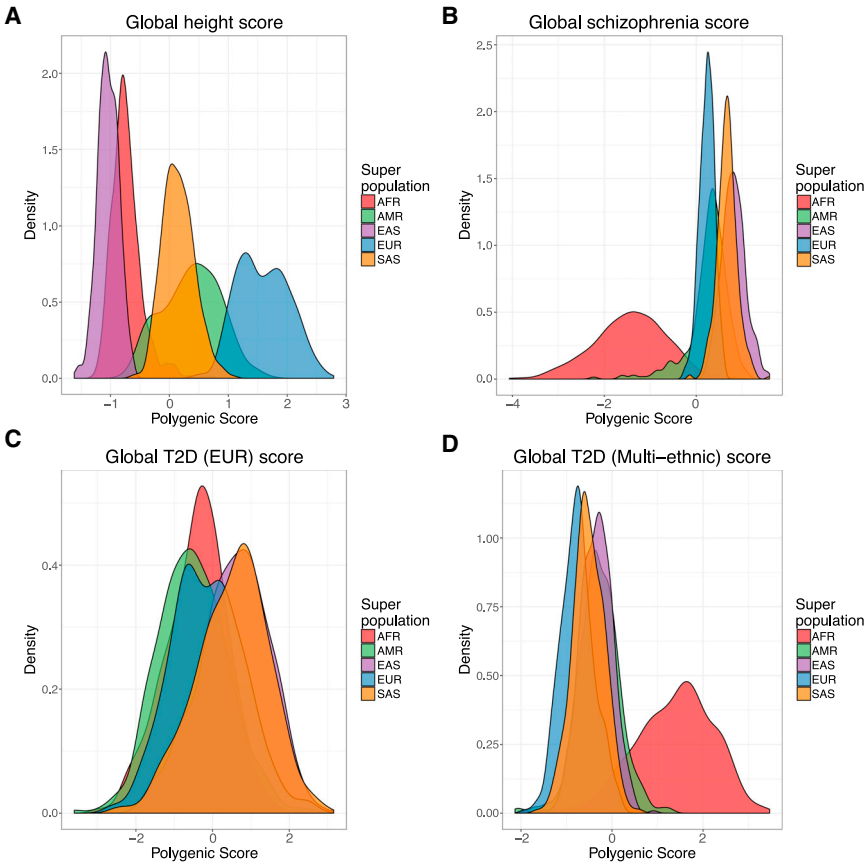

Figure 4. Biased Genetic Discoveries Influence Disease Risk Inferences
Inferred and standardized polygenic risk scores across all individuals and colored by population for (A) height based on summary statistics from Wood et al.,[10] (B) schizophrenia based on summary statistics from the Schizophrenia Working Group of the Psychiatric Genomics Consortium,[11] (C) type II diabetes summary statistics derived from a European cohort from Gaulton et al.,[86] and (D) type II diabetes summary statistics derived from a multi-ethnic cohort from Mahajan et al.[87]

We find that the correlation between true and inferred polygenic risk is generally low (Figures 5C and S13), consistent with limited variance explained by polygenic risk scores from GWASs of these cohort sizes for height (e.g., ~10% of variance explained for a cohort of size 183,727[63]) and schizophrenia (e.g., ~7% variance explained for a cohort of size 36,989 case subjects and 113,075 control subjects[11]). Low correlations in our simulations are most likely because common tag variants are a poor proxy for rare causal variants. As expected, correlations between true and inferred risk within populations are typically highest in the European population (i.e., the population in which variants were discovered, Figures 5A and S13). To quantify the differential prediction accuracy of polygenic risk scores across populations, we also evaluate the log odds ratio of being a case subject compared to a control subject across deciles of inferred polygenic risk in each population. We identify greater power to discern between case and control subjects in the EUR discovery population relative to the AFR and EAS populations (i.e., more heritable variation explained, as evidenced by a steeper slope) (Figure S14B). Across all populations, the mean Spearman correlations between true and inferred polygenic risk increase with increasing heritability while the standard deviations of these correlations significantly decrease ($p = 0.05$); however, there is considerable within-population heterogeneity resulting in high variation in scores across all populations. We find that in these neutral simulations, a polygenic risk score bias in essentially any direction is possible even when choosing the exact same causal variants and heritability and varying only fixed effect size (i.e., inferred polygenic risk in Europeans can be higher, lower, or intermediate compared to true risk relative to East Asians or Africans, Figures S12 and 5B).

Discussion

To date, GWASs have been performed opportunistically in primarily single-ancestry European cohorts, and an open question remains about their biomedical relevance for disease associations in other ancestries. As studies gain power by increasing sample sizes, effect size estimates become more precise and novel associations at lower frequencies are feasible. However, rare variants are largely population-private, and their effects are unlikely to transfer to new populations. Because linkage disequilibrium and allele frequencies vary across ancestries, effect size estimates from diverse cohorts are typically more precise than from single-ancestry cohorts (and often tempered),[5] and the resolution of causal variant fine-mapping is considerably improved.[87] Across a range of genetic architectures, diverse cohorts provide the opportunity to reduce false positives. At the Mendelian end of the spectrum, for example, disentangling risk variants with incomplete penetrance from benign false positives and localizing functional effects in genes is much more feasible with large diverse population cohorts than with single-ancestry analyses.[94] Multiple false positive reports of pathogenic variants causing hypertrophic cardiomyopathy, a disease with relatively simple genomic architecture, have been returned to individuals of African descent or unspecified ancestry that would have been prevented if even a small number of African American samples were included in control cohorts.[9] At the highly complex end of the polygenicity spectrum, we and others have shown that the utility of polygenic risk inferences and

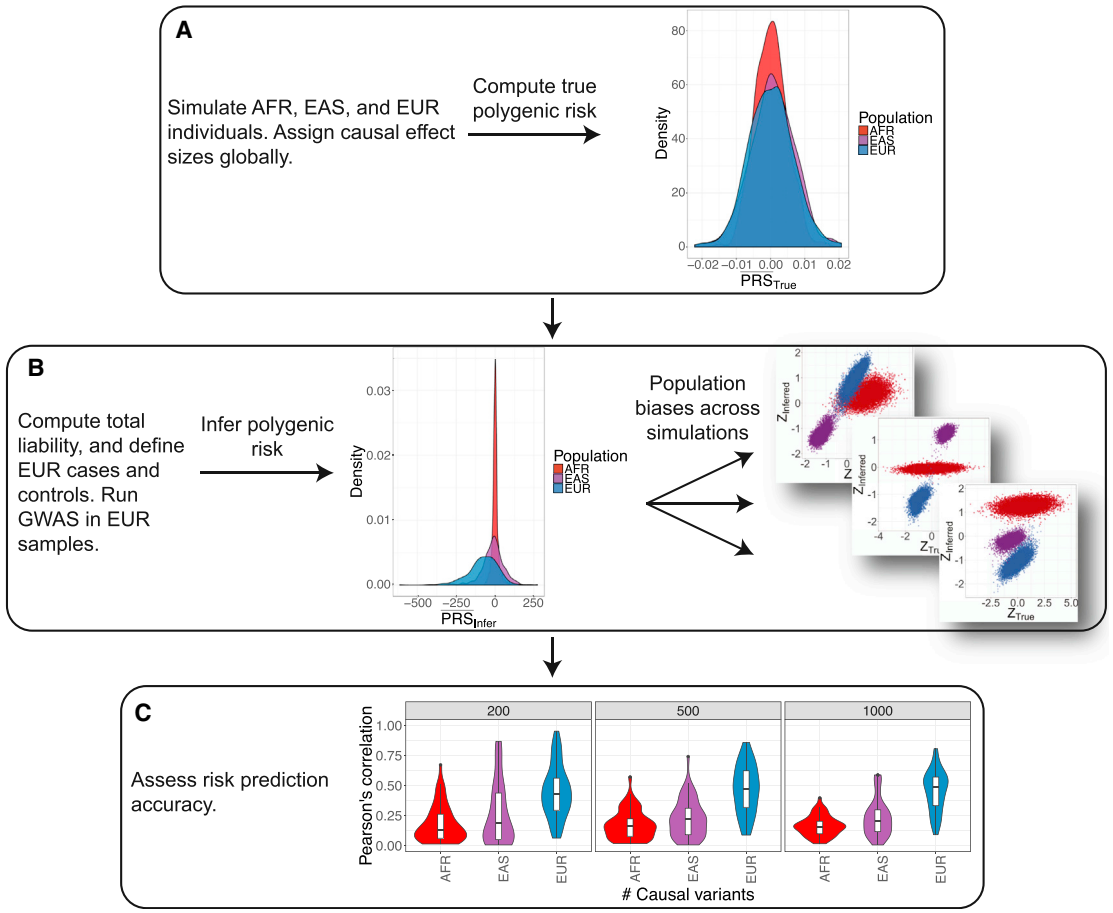

Figure 5. Coalescent Simulation Framework to Generate True and Inferred Polygenic Risk Scores
Results of true and inferred polygenic risk scores, as well as their correlation, were computed via GWAS summary statistics from 10,000 simulated EUR case and control subjects modeling European, East Asian, and African population history (demographic parameters are from Gravel et al.[14]).
(A) The distribution of mean true, unstandardized polygenic risk scores for each population across 500 simulations with $m = 1{,}000$ causal variants and $h^2 = 0.67$.
(B) The distribution of mean inferred, unstandardized polygenic risk for the same simulation parameters as in (A) (center) and standardized true versus inferred polygenic risk scores for three different coalescent simulation replicates showing 10,000 randomly drawn samples from each population not included as case or control subjects (right).
(C) Violin plots show Pearson's correlation across 50 iterations per parameter set between true and inferred polygenic risk scores across differing genetic architectures, including $m = 200$, 500, and 1,000 causal variants and $h^2 = 0.67$.

the heritable phenotypic variance explained in diverse populations is improved with more diverse cohorts.[92,95]

Standard single-ancestry GWASs typically apply linear mixed model approaches and/or incorporate principal components as covariates to control for confounding from population structure with primarily European-descent cohorts.[1–3] A key concern when including multiple diverse populations in a GWAS is that there is increasing likelihood of identifying false positive variants associated with disease that are driven by allele frequency differences across ancestries. However, previous studies have analyzed association data for diverse ancestries and replicated findings across ethnicities, assuaging these concerns.[6,87] In this study, we show that this ancestry stratification is not continuous along the genome: long tracts of ancestrally diverse populations present in admixed samples from the Americas are easily and accurately detected. Querying population substructure within these tracts recapitulates expected trends, e.g., European ancestry in African Americans primarily descends from northern Europeans in contrast to European ancestry from Hispanic/Latinos, which primarily descends from southern Europeans, as seen previously.[44] Additionally, population substructure follows a north-south cline in the Native component of Hispanic/Latinos, and the African component of admixed African descent populations in the Americas most closely resembles reference populations from Nigeria (notwithstanding the limited set of African populations from the 1000 Genomes Project). Admixture mapping has been successful at large sample sizes for identifying ancestry-specific genetic risk factors for disease.[30] Given the level of accuracy and subcontinental resolution attained with local ancestry tracts in admixed populations, we emphasize the utility

of a unified framework to jointly analyze genetic associations with local ancestry simultaneously.[40]

The transferability of GWASs is aided by the inclusion of diverse populations.[96] We have shown that European discovery biases in GWASs are recapitulated in local ancestry tracts in admixed samples. We have quantified GWAS study biases in ancestral populations and shown that GWAS variants are at lower frequency specifically within African and Native tracts and higher frequency in European tracts in admixed American populations. Imputation accuracy is also stratified across diverged ancestries, including across local ancestries in admixed populations. With decreased imputation accuracy especially on Native American tracts, there is decreased power for potential ancestry-specific associations. This differentially limits conclusions for GWASs in an admixed population in a two-pronged manner: the ability to capture variation and the power to estimate associations.

As GWASs scale to sample sizes on the order of hundreds of thousands to millions, genetic risk prediction accuracy at the individual level improves.[59] However, we show that the utility of polygenic risk scores computed using GWAS summary statistics are dependent on genetic similarity to the discovery cohort. Best linear unbiased prediction (BLUP) methods have been proposed to improve risk scores, but they require access to raw genetic data typically from very large datasets, are also dependent on LD structure in the study population, and offer only modest improvements in prediction accuracy.[52] Furthermore, polygenic risk scores (PRSs) contain a mix of true positives (which have the bias described above) and false positives in the training GWAS. False positives, being chance statistical fluctuations, do not have the same allele frequency bias and therefore unfortunately play an outsized role in applying a PRS in a new population.

We have demonstrated that polygenic risk scores computed via current standard methods with summary statistics from a single-ancestry discovery cohort have numerous problems: differences in polygenic risk scores across populations are significant but not supported by epidemiological or anthropometric studies of the same traits, and directionality biases in polygenic risk scores across populations are unpredictable. Our coalescent simulations recapitulate these results and show that across replicates (i.e., traits, and thus not necessarily within a single trait), cross-population prediction accuracy is diminished with increasing divergence from the discovery cohort. These simulations provide further insight into directional inconsistencies in inferred polygenic risk scores with the same demographic model across replicate simulations, indicating that different traits are likely to suffer from biases that cannot be adjusted, e.g., using prinicipal components alone. Directional selection is expected to bias polygenic risk inferences even more. Because biases arise from genetic drift alone, we recommend (1) avoiding interpretations from polygenic risk score differences extrapolated across populations, as these are likely confounded by latent population structure that is not properly corrected for with current standard methods, (2) mean-centering polygenic risk scores for each population, and (3) computing polygenic risk scores in populations with similar demographic histories as the study sample to ensure maximal predictive power. Further, additional methods that account for local ancestry in genetic risk prediction to incorporate different ancestral linkage disequilibrium and allele frequencies are needed. This study demonstrates the utility of disentangling ancestry tracts in recently admixed populations for inferring recent demographic history and identifying ancestry-stratified analytical biases; we also motivate the need to include more ancestrally diverse cohorts in GWASs to ensure that health disparities arising from genetic risk prediction do not become pervasive in individuals of admixed and non-European descent.

Supplemental Data

Supplemental Data include 14 figures and 4 tables and can be found with this article online at http://dx.doi.org/10.1016/j.ajhg.2017.03.004.

Conflicts of Interest

C.D.B. is a member of the scientific advisory boards for Liberty Biosecurity, Personalis, 23andMe Roots into the Future, Ancestry.com, IdentifyGenomics, and Etalon and is a founder of CDB Consulting. C.R.G. owns stock in 23andMe. M.J.D. is a member the scientific advisory board for Ancestry.com. E.E.K. and C.R.G. are members of the scientific advisory board for Encompass Biosciences. E.E.K. consults for Illumina. B.M.N. is a member of the scientific advisory board for Deep Genomics.

Acknowledgments

We thank Suyash Shringarpure, Brian Maples, Andres Moreno-Estrada, Danny Park, Noah Zaitlen, Alexander Gusev, and Alkes Price for helpful discussions/feedback. We thank Verneri Antilla for providing GWAS summary statistics. We thank Jerome Kelleher for several conversations about msprime, providing example scripts, and implementing new simulation capabilities. This work was supported by funds from several grants: the National Human Genome Research Institute under award numbers U01HG009080 (E.E.K., C.D.B., C.R.G.), U01HG007419 (C.D.B., C.R.G., G.L.W.), U01HG007417 (E.E.K.), U01HG005208 (M.J.D.), T32HG000044 (C.R.G.), and R01GM083606 (C.D.B.), the National Institute of General Medical Sciences under award number T32GM007790 (A.R.M.) at the National Institute of Health, the National Institute for Mental Health 5U01MH094432-02 (R.G.W., M.J.D.), the Directorate of Mathematical and Physical Sciences award 1201234 (S.G., C.D.B.) at the National Science Foundation, the Canadian Institutes of Health Research through the Canada Research Chair program and operating grant MOP-136855 (S.G.), and a Sloan Research Fellowship (S.G.).

Received: November 23, 2016
Accepted: March 10, 2017
Published: March 30, 2017

Web Resources

ancestry_pipeline, https://github.com/armartin/ancestry_pipeline/
Local ancestry calls, https://personal.broadinstitute.org/armartin/tgp_admixture/
msprime, https://github.com/jeromekelleher/msprime
PCAmask, https://sites.google.com/site/pcamask/dowload
Phased 1000 Genomes haplotypes, ftp://ftp-trace.ncbi.nih.gov/1000genomes/ftp/release/20130502/supporting/shapeit2_scaffolds/wgs_gt_scaffolds/
Tracts, https://github.com/sgravel/tracts

References

1. Need, A.C., and Goldstein, D.B. (2009). Next generation disparities in human genomics: concerns and remedies. Trends Genet. *25*, 489–494.
2. Bustamante, C.D., Burchard, E.G., and De la Vega, F.M. (2011). Genomics for the world. Nature *475*, 163–165.
3. Petrovski, S., and Goldstein, D.B. (2016). Unequal representation of genetic variation across ancestry groups creates healthcare inequality in the application of precision medicine. Genome Biol. *17*, 157.
4. Popejoy, A.B., and Fullerton, S.M. (2016). Genomics is failing on diversity. Nature *538*, 161–164.
5. Carlson, C.S., Matise, T.C., North, K.E., Haiman, C.A., Fesinmeyer, M.D., Buyske, S., Schumacher, F.R., Peters, U., Franceschini, N., Ritchie, M.D., et al.; PAGE Consortium (2013). Generalization and dilution of association results from European GWAS in populations of non-European ancestry: the PAGE study. PLoS Biol. *11*, e1001661.
6. Waters, K.M., Stram, D.O., Hassanein, M.T., Le Marchand, L., Wilkens, L.R., Maskarinec, G., Monroe, K.R., Kolonel, L.N., Altshuler, D., Henderson, B.E., and Haiman, C.A. (2010). Consistent association of type 2 diabetes risk variants found in europeans in diverse racial and ethnic groups. PLoS Genet. *6*, 6.
7. Hindorff, L.A., Sethupathy, P., Junkins, H.A., Ramos, E.M., Mehta, J.P., Collins, F.S., and Manolio, T.A. (2009). Potential etiologic and functional implications of genome-wide association loci for human diseases and traits. Proc. Natl. Acad. Sci. USA *106*, 9362–9367.
8. Scutari, M., Mackay, I., and Balding, D. (2016). Using genetic distance to infer the accuracy of genomic prediction. PLoS Genet. *12*, e1006288.
9. Manrai, A.K., Funke, B.H., Rehm, H.L., Olesen, M.S., Maron, B.A., Szolovits, P., Margulies, D.M., Loscalzo, J., and Kohane, I.S. (2016). Genetic misdiagnoses and the potential for health disparities. N. Engl. J. Med. *375*, 655–665.
10. Wood, A.R., Esko, T., Yang, J., Vedantam, S., Pers, T.H., Gustafsson, S., Chu, A.Y., Estrada, K., Luan, J., Kutalik, Z., et al.; Electronic Medical Records and Genomics (eMEMERGEGE) Consortium; MIGen Consortium; PAGEGE Consortium; and LifeLines Cohort Study (2014). Defining the role of common variation in the genomic and biological architecture of adult human height. Nat. Genet. *46*, 1173–1186.
11. Schizophrenia Working Group of the Psychiatric Genomics Consortium (2014). Biological insights from 108 schizophrenia-associated genetic loci. Nature *511*, 421–427.
12. Muñoz, M., Pong-Wong, R., Canela-Xandri, O., Rawlik, K., Haley, C.S., and Tenesa, A. (2016). Evaluating the contribution of genetics and familial shared environment to common disease using the UK Biobank. Nat. Genet. *48*, 980–983.
13. Mathieson, I., and McVean, G. (2012). Differential confounding of rare and common variants in spatially structured populations. Nat. Genet. *44*, 243–246.
14. Gravel, S., Henn, B.M., Gutenkunst, R.N., Indap, A.R., Marth, G.T., Clark, A.G., Yu, F., Gibbs, R.A., Bustamante, C.D.; and 1000 Genomes Project (2011). Demographic history and rare allele sharing among human populations. Proc. Natl. Acad. Sci. USA *108*, 11983–11988.
15. Walter, K., Min, J.L., Huang, J., Crooks, L., Memari, Y., McCarthy, S., Perry, J.R., Xu, C., Futema, M., Lawson, D., et al.; UK10K Consortium (2015). The UK10K project identifies rare variants in health and disease. Nature *526*, 82–90.
16. Novembre, J., Johnson, T., Bryc, K., Kutalik, Z., Boyko, A.R., Auton, A., Indap, A., King, K.S., Bergmann, S., Nelson, M.R., et al. (2008). Genes mirror geography within Europe. Nature *456*, 98–101.
17. Do, R., Kathiresan, S., and Abecasis, G.R. (2012). Exome sequencing and complex disease: practical aspects of rare variant association studies. Hum. Mol. Genet. *21* (R1), R1–R9.
18. Lek, M., Karczewski, K.J., Minikel, E.V., Samocha, K.E., Banks, E., Fennell, T., O'Donnell-Luria, A.H., Ware, J.S., Hill, A.J., Cummings, B.B., et al.; Exome Aggregation Consortium (2016). Analysis of protein-coding genetic variation in 60,706 humans. Nature *536*, 285–291.
19. Auton, A., Brooks, L.D., Durbin, R.M., Garrison, E.P., Kang, H.M., Korbel, J.O., Marchini, J.L., McCarthy, S., McVean, G.A., Abecasis, G.R.; and 1000 Genomes Project Consortium (2015). A global reference for human genetic variation. Nature *526*, 68–74.
20. Tennessen, J.A., Bigham, A.W., O'Connor, T.D., Fu, W., Kenny, E.E., Gravel, S., McGee, S., Do, R., Liu, X., Jun, G., et al.; Broad GO; Seattle GO; and NHLBI Exome Sequencing Project (2012). Evolution and functional impact of rare coding variation from deep sequencing of human exomes. Science *337*, 64–69.
21. Grossman, S.R., Shlyakhter, I., Karlsson, E.K., Byrne, E.H., Morales, S., Frieden, G., Hostetter, E., Angelino, E., Garber, M., Zuk, O., et al. (2010). A composite of multiple signals distinguishes causal variants in regions of positive selection. Science *327*, 883–886.
22. MacArthur, D.G., Balasubramanian, S., Frankish, A., Huang, N., Morris, J., Walter, K., Jostins, L., Habegger, L., Pickrell, J.K., Montgomery, S.B., et al.; 1000 Genomes Project Consortium (2012). A systematic survey of loss-of-function variants in human protein-coding genes. Science *335*, 823–828.
23. Lohmueller, K.E., Indap, A.R., Schmidt, S., Boyko, A.R., Hernandez, R.D., Hubisz, M.J., Sninsky, J.J., White, T.J., Sunyaev, S.R., Nielsen, R., et al. (2008). Proportionally more deleterious genetic variation in European than in African populations. Nature *451*, 994–997.
24. Fu, W., Gittelman, R.M., Bamshad, M.J., and Akey, J.M. (2014). Characteristics of neutral and deleterious protein-coding variation among individuals and populations. Am. J. Hum. Genet. *95*, 421–436.
25. Simons, Y.B., Turchin, M.C., Pritchard, J.K., and Sella, G. (2014). The deleterious mutation load is insensitive to recent population history. Nat. Genet. *46*, 220–224.
26. Price, A.L., Tandon, A., Patterson, N., Barnes, K.C., Rafaels, N., Ruczinski, I., Beaty, T.H., Mathias, R., Reich, D., and Myers, S. (2009). Sensitive detection of chromosomal segments of distinct ancestry in admixed populations. PLoS Genet. *5*, e1000519.

27. Pasaniuc, B., Zaitlen, N., Lettre, G., Chen, G.K., Tandon, A., Kao, W.H.L., Ruczinski, I., Fornage, M., Siscovick, D.S., Zhu, X., et al. (2011). Enhanced statistical tests for GWAS in admixed populations: assessment using African Americans from CARe and a Breast Cancer Consortium. PLoS Genet. *7*, e1001371.
28. Fejerman, L., Chen, G.K., Eng, C., Huntsman, S., Hu, D., Williams, A., Pasaniuc, B., John, E.M., Via, M., Gignoux, C., et al. (2012). Admixture mapping identifies a locus on 6q25 associated with breast cancer risk in US Latinas. Hum. Mol. Genet. *21*, 1907–1917.
29. Fejerman, L., Ahmadiyeh, N., Hu, D., Huntsman, S., Beckman, K.B., Caswell, J.L., Tsung, K., John, E.M., Torres-Mejia, G., Carvajal-Carmona, L., et al.; COLUMBUS Consortium (2014). Genome-wide association study of breast cancer in Latinas identifies novel protective variants on 6q25. Nat. Commun. *5*, 5260.
30. Freedman, M.L., Haiman, C.A., Patterson, N., McDonald, G.J., Tandon, A., Waliszewska, A., Penney, K., Steen, R.G., Ardlie, K., John, E.M., et al. (2006). Admixture mapping identifies 8q24 as a prostate cancer risk locus in African-American men. Proc. Natl. Acad. Sci. USA *103*, 14068–14073.
31. Bhatia, G., Patterson, N., Pasaniuc, B., Zaitlen, N., Genovese, G., Pollack, S., Mallick, S., Myers, S., Tandon, A., Spencer, C., et al. (2011). Genome-wide comparison of African-ancestry populations from CARe and other cohorts reveals signals of natural selection. Am. J. Hum. Genet. *89*, 368–381.
32. Moreno-Estrada, A., Gravel, S., Zakharia, F., McCauley, J.L., Byrnes, J.K., Gignoux, C.R., Ortiz-Tello, P.A., Martínez, R.J., Hedges, D.J., Morris, R.W., et al. (2013). Reconstructing the population genetic history of the Caribbean. PLoS Genet. *9*, e1003925.
33. Bryc, K., Velez, C., Karafet, T., Moreno-Estrada, A., Reynolds, A., Auton, A., Hammer, M., Bustamante, C.D., and Ostrer, H. (2010). Colloquium paper: genome-wide patterns of population structure and admixture among Hispanic/Latino populations. Proc. Natl. Acad. Sci. USA *107* (*Suppl 2*), 8954–8961.
34. Pritchard, J.K., Stephens, M., and Donnelly, P. (2000). Inference of population structure using multilocus genotype data. Genetics *155*, 945–959.
35. Tang, H., Peng, J., Wang, P., and Risch, N.J. (2005). Estimation of individual admixture: analytical and study design considerations. Genet. Epidemiol. *28*, 289–301.
36. Alexander, D.H., Novembre, J., and Lange, K. (2009). Fast model-based estimation of ancestry in unrelated individuals. Genome Res. *19*, 1655–1664.
37. Price, A.L., Zaitlen, N.A., Reich, D., and Patterson, N. (2010). New approaches to population stratification in genome-wide association studies. Nat. Rev. Genet. *11*, 459–463.
38. Mathieson, I., and McVean, G. (2014). Demography and the age of rare variants. PLoS Genet. *10*, e1004528.
39. O'Connor, T.D., Fu, W., Mychaleckyj, J.C., Logsdon, B., Auer, P., Carlson, C.S., Leal, S.M., Smith, J.D., Rieder, M.J., Bamshad, M.J., et al.; NHLBI GO Exome Sequencing Project; and ESP Population Genetics and Statistical Analysis Working Group, Emily Turner (2015). Rare variation facilitates inferences of fine-scale population structure in humans. Mol. Biol. Evol. *32*, 653–660.
40. Szulc, P., Bogdan, M., Frommlet, F., and Tang, H. (2016). Joint genotype- and ancestry-based genome-wide association studies in admixed populations. bioRxiv. http://dx.doi.org/10.1101/062554.
41. Conomos, M.P., Reiner, A.P., Weir, B.S., and Thornton, T.A. (2016). Model-free estimation of recent genetic relatedness. Am. J. Hum. Genet. *98*, 127–148.
42. Zaitlen, N., Paşaniuc, B., Gur, T., Ziv, E., and Halperin, E. (2010). Leveraging genetic variability across populations for the identification of causal variants. Am. J. Hum. Genet. *86*, 23–33.
43. Genovese, G., Handsaker, R.E., Li, H., Kenny, E.E., and McCarroll, S.A. (2013). Mapping the human reference genome's missing sequence by three-way admixture in Latino genomes. Am. J. Hum. Genet. *93*, 411–421.
44. Baharian, S., Barakatt, M., Gignoux, C.R., Shringarpure, S., Errington, J., Blot, W.J., Bustamante, C.D., Kenny, E.E., Williams, S.M., Aldrich, M.C., and Gravel, S. (2016). The great migration and African-American genomic diversity. PLoS Genet. *12*, e1006059.
45. Reich, D., Patterson, N., Campbell, D., Tandon, A., Mazieres, S., Ray, N., Parra, M.V., Rojas, W., Duque, C., Mesa, N., et al. (2012). Reconstructing Native American population history. Nature *488*, 370–374.
46. Ruiz-Linares, A., Adhikari, K., Acuña-Alonzo, V., Quinto-Sanchez, M., Jaramillo, C., Arias, W., Fuentes, M., Pizarro, M., Everardo, P., de Avila, F., et al. (2014). Admixture in Latin America: geographic structure, phenotypic diversity and self-perception of ancestry based on 7,342 individuals. PLoS Genet. *10*, e1004572.
47. Moreno-Estrada, A., Gignoux, C.R., Fernández-López, J.C., Zakharia, F., Sikora, M., Contreras, A.V., Acuña-Alonzo, V., Sandoval, K., Eng, C., Romero-Hidalgo, S., et al. (2014). Human genetics. The genetics of Mexico recapitulates Native American substructure and affects biomedical traits. Science *344*, 1280–1285.
48. Purcell, S.M., Wray, N.R., Stone, J.L., Visscher, P.M., O'Donovan, M.C., Sullivan, P.F., Sklar, P.; and International Schizophrenia Consortium (2009). Common polygenic variation contributes to risk of schizophrenia and bipolar disorder. Nature *460*, 748–752.
49. Yang, J., Benyamin, B., McEvoy, B.P., Gordon, S., Henders, A.K., Nyholt, D.R., Madden, P.A., Heath, A.C., Martin, N.G., Montgomery, G.W., et al. (2010). Common SNPs explain a large proportion of the heritability for human height. Nat. Genet. *42*, 565–569.
50. Yang, J., Weedon, M.N., Purcell, S., Lettre, G., Estrada, K., Willer, C.J., Smith, A.V., Ingelsson, E., O'Connell, J.R., Mangino, M., et al.; GIANT Consortium (2011). Genomic inflation factors under polygenic inheritance. Eur. J. Hum. Genet. *19*, 807–812.
51. Wray, N.R., Goddard, M.E., and Visscher, P.M. (2007). Prediction of individual genetic risk to disease from genome-wide association studies. Genome Res. *17*, 1520–1528.
52. Wray, N.R., Yang, J., Hayes, B.J., Price, A.L., Goddard, M.E., and Visscher, P.M. (2013). Pitfalls of predicting complex traits from SNPs. Nat. Rev. Genet. *14*, 507–515.
53. Wray, N.R., Lee, S.H., Mehta, D., Vinkhuyzen, A.A., Dudbridge, F., and Middeldorp, C.M. (2014). Research review: polygenic methods and their application to psychiatric traits. J. Child Psychol. Psychiatry *55*, 1068–1087.
54. Chatterjee, N., Shi, J., and García-Closas, M. (2016). Developing and evaluating polygenic risk prediction models for stratified disease prevention. Nat. Rev. Genet. *17*, 392–406.
55. Dudbridge, F. (2016). Polygenic epidemiology. Genet. Epidemiol. *40*, 268–272.

56. So, H.C., and Sham, P.C. (2017). Exploring the predictive power of polygenic scores derived from genome-wide association studies: a study of 10 complex traits. Bioinformatics *33*, 886–892.
57. Euesden, J., Lewis, C.M., and O'Reilly, P.F. (2015). PRSice: polygenic risk score software. Bioinformatics *31*, 1466–1468.
58. Shi, J., Park, J.H., Duan, J., Berndt, S.T., Moy, W., Yu, K., Song, L., Wheeler, W., Hua, X., Silverman, D., et al.; MGS (Molecular Genetics of Schizophrenia) GWAS Consortium; GECCO (The Genetics and Epidemiology of Colorectal Cancer Consortium); GAME-ON/TRICL (Transdisciplinary Research in Cancer of the Lung) GWAS Consortium; PRACTICAL (PRostate cancer AssoCiation group To Investigate Cancer Associated aLterations) Consortium; PanScan Consortium; and GAME-ON/ELLIPSE Consortium (2016). Winner's curse correction and variable thresholding improve performance of polygenic risk modeling based on genome-wide association study summary-level data. PLoS Genet. *12*, e1006493.
59. Dudbridge, F. (2013). Power and predictive accuracy of polygenic risk scores. PLoS Genet. *9*, e1003348.
60. Pharoah, P.D., Antoniou, A.C., Easton, D.F., and Ponder, B.A. (2008). Polygenes, risk prediction, and targeted prevention of breast cancer. N. Engl. J. Med. *358*, 2796–2803.
61. Evans, D.M., Visscher, P.M., and Wray, N.R. (2009). Harnessing the information contained within genome-wide association studies to improve individual prediction of complex disease risk. Hum. Mol. Genet. *18*, 3525–3531.
62. Okbay, A., Beauchamp, J.P., Fontana, M.A., Lee, J.J., Pers, T.H., Rietveld, C.A., Turley, P., Chen, G.B., Emilsson, V., Meddens, S.F., et al.; LifeLines Cohort Study (2016). Genome-wide association study identifies 74 loci associated with educational attainment. Nature *533*, 539–542.
63. Lango Allen, H., Estrada, K., Lettre, G., Berndt, S.I., Weedon, M.N., Rivadeneira, F., Willer, C.J., Jackson, A.U., Vedantam, S., Raychaudhuri, S., et al. (2010). Hundreds of variants clustered in genomic loci and biological pathways affect human height. Nature *467*, 832–838.
64. Bush, W.S., Sawcer, S.J., de Jager, P.L., Oksenberg, J.R., McCauley, J.L., Pericak-Vance, M.A., Haines, J.L.; and International Multiple Sclerosis Genetics Consortium (IMSGC) (2010). Evidence for polygenic susceptibility to multiple sclerosis–the shape of things to come. Am. J. Hum. Genet. *86*, 621–625.
65. Stahl, E.A., Wegmann, D., Trynka, G., Gutierrez-Achury, J., Do, R., Voight, B.F., Kraft, P., Chen, R., Kallberg, H.J., Kurreeman, F.A., et al.; Diabetes Genetics Replication and Meta-analysis Consortium; and Myocardial Infarction Genetics Consortium (2012). Bayesian inference analyses of the polygenic architecture of rheumatoid arthritis. Nat. Genet. *44*, 483–489.
66. Maier, R., Moser, G., Chen, G.B., Ripke, S., Coryell, W., Potash, J.B., Scheftner, W.A., Shi, J., Weissman, M.M., Hultman, C.M., et al.; Cross-Disorder Working Group of the Psychiatric Genomics Consortium (2015). Joint analysis of psychiatric disorders increases accuracy of risk prediction for schizophrenia, bipolar disorder, and major depressive disorder. Am. J. Hum. Genet. *96*, 283–294.
67. Vilhjálmsson, B.J., Yang, J., Finucane, H.K., Gusev, A., Lindström, S., Ripke, S., Genovese, G., Loh, P.R., Bhatia, G., Do, R., et al.; Schizophrenia Working Group of the Psychiatric Genomics Consortium, Discovery, Biology, and Risk of Inherited Variants in Breast Cancer (DRIVE) study (2015). Modeling linkage disequilibrium increases accuracy of polygenic risk scores. Am. J. Hum. Genet. *97*, 576–592.
68. Chen, H., Hey, J., and Slatkin, M. (2015). A hidden Markov model for investigating recent positive selection through haplotype structure. Theor. Popul. Biol. *99*, 18–30.
69. Mao, X., Bigham, A.W., Mei, R., Gutierrez, G., Weiss, K.M., Brutsaert, T.D., Leon-Velarde, F., Moore, L.G., Vargas, E., McKeigue, P.M., et al. (2007). A genomewide admixture mapping panel for Hispanic/Latino populations. Am. J. Hum. Genet. *80*, 1171–1178.
70. O'Connell, J., Gurdasani, D., Delaneau, O., Pirastu, N., Ulivi, S., Cocca, M., Traglia, M., Huang, J., Huffman, J.E., Rudan, I., et al. (2014). A general approach for haplotype phasing across the full spectrum of relatedness. PLoS Genet. *10*, e1004234.
71. Maples, B.K., Gravel, S., Kenny, E.E., and Bustamante, C.D. (2013). RFMix: a discriminative modeling approach for rapid and robust local-ancestry inference. Am. J. Hum. Genet. *93*, 278–288.
72. Gravel, S. (2012). Population genetics models of local ancestry. Genetics *191*, 607–619.
73. Abecasis, G.R., Auton, A., Brooks, L.D., DePristo, M.A., Durbin, R.M., Handsaker, R.E., Kang, H.M., Marth, G.T., McVean, G.A.; and 1000 Genomes Project Consortium (2012). An integrated map of genetic variation from 1,092 human genomes. Nature *491*, 56–65.
74. Purcell, S., Neale, B., Todd-Brown, K., Thomas, L., Ferreira, M.A., Bender, D., Maller, J., Sklar, P., de Bakker, P.I., Daly, M.J., and Sham, P.C. (2007). PLINK: a tool set for whole-genome association and population-based linkage analyses. Am. J. Hum. Genet. *81*, 559–575.
75. Kelleher, J., Etheridge, A.M., and McVean, G. (2016). Efficient coalescent simulation and genealogical analysis for large sample sizes. PLoS Comput. Biol. *12*, e1004842.
76. Mathias, R.A., Taub, M.A., Gignoux, C.R., Fu, W., Musharoff, S., O'Connor, T.D., Vergara, C., Torgerson, D.G., Pino-Yanes, M., Shringarpure, S.S., et al.; CAAPA (2016). A continuum of admixture in the Western Hemisphere revealed by the African Diaspora genome. Nat. Commun. *7*, 12522.
77. Shringarpure, S.S., Bustamante, C.D., Lange, K.L., and Alexander, D.H. (2016). Efficient analysis of large datasets and sex bias with ADMIXTURE. bioRxiv. http://dx.doi.org/10.1101/039347.
78. Price, A.L., Patterson, N.J., Plenge, R.M., Weinblatt, M.E., Shadick, N.A., and Reich, D. (2006). Principal components analysis corrects for stratification in genome-wide association studies. Nat. Genet. *38*, 904–909.
79. Baran, Y., Pasaniuc, B., Sankararaman, S., Torgerson, D.G., Gignoux, C., Eng, C., Rodriguez-Cintron, W., Chapela, R., Ford, J.G., Avila, P.C., et al. (2012). Fast and accurate inference of local ancestry in Latino populations. Bioinformatics *28*, 1359–1367.
80. Tishkoff, S.A., Reed, F.A., Friedlaender, F.R., Ehret, C., Ranciaro, A., Froment, A., Hirbo, J.B., Awomoyi, A.A., Bodo, J.M., Doumbo, O., et al. (2009). The genetic structure and history of Africans and African Americans. Science *324*, 1035–1044.
81. Zakharia, F., Basu, A., Absher, D., Assimes, T.L., Go, A.S., Hlatky, M.A., Iribarren, C., Knowles, J.W., Li, J., Narasimhan, B., et al. (2009). Characterizing the admixed African ancestry of African Americans. Genome Biol. *10*, R141.
82. Schroeder, H., Ávila-Arcos, M.C., Malaspinas, A.S., Poznik, G.D., Sandoval-Velasco, M., Carpenter, M.L., Moreno-Mayar, J.V., Sikora, M., Johnson, P.L., Allentoft, M.E., et al. (2015).

Genome-wide ancestry of 17th-century enslaved Africans from the Caribbean. Proc. Natl. Acad. Sci. USA *112*, 3669–3673.

83. Gravel, S., Zakharia, F., Moreno-Estrada, A., Byrnes, J.K., Muzzio, M., Rodriguez-Flores, J.L., Kenny, E.E., Gignoux, C.R., Maples, B.K., Guiblet, W., et al.; 1000 Genomes Project (2013). Reconstructing Native American migrations from whole-genome and whole-exome data. PLoS Genet. *9*, e1004023.
84. Kessler, M.D., Yerges-Armstrong, L., Taub, M.A., Shetty, A.C., Maloney, K., Jeng, L.J.B., Ruczinski, I., Levin, A.M., Williams, L.K., Beaty, T.H., et al.; Consortium on Asthma among African-ancestry Populations in the Americas (CAAPA) (2016). Challenges and disparities in the application of personalized genomic medicine to populations with African ancestry. Nat. Commun. *7*, 12521.
85. Shungin, D., Winkler, T.W., Croteau-Chonka, D.C., Ferreira, T., Locke, A.E., Mägi, R., Strawbridge, R.J., Pers, T.H., Fischer, K., Justice, A.E., et al.; ADIPOGen Consortium; CARDIOGRAMplusC4D Consortium; CKDGen Consortium; GEFOS Consortium; GENIE Consortium; GLGC; ICBP; International Endogene Consortium; LifeLines Cohort Study; MAGIC Investigators; MuTHER Consortium; PAGE Consortium; and ReproGen Consortium (2015). New genetic loci link adipose and insulin biology to body fat distribution. Nature *518*, 187–196.
86. Gaulton, K.J., Ferreira, T., Lee, Y., Raimondo, A., Mägi, R., Reschen, M.E., Mahajan, A., Locke, A., Rayner, N.W., Robertson, N., et al.; DIAbetes Genetics Replication And Meta-analysis (DIAGRAM) Consortium (2015). Genetic fine mapping and genomic annotation defines causal mechanisms at type 2 diabetes susceptibility loci. Nat. Genet. *47*, 1415–1425.
87. Mahajan, A., Go, M.J., Zhang, W., Below, J.E., Gaulton, K.J., Ferreira, T., Horikoshi, M., Johnson, A.D., Ng, M.C., Prokopenko, I., et al.; DIAbetes Genetics Replication And Meta-analysis (DIAGRAM) Consortium; Asian Genetic Epidemiology Network Type 2 Diabetes (AGEN-T2D) Consortium; South Asian Type 2 Diabetes (SAT2D) Consortium; Mexican American Type 2 Diabetes (MAT2D) Consortium; and Type 2 Diabetes Genetic Exploration by Nex-generation sequencing in muylti-Ethnic Samples (T2D-GENES) Consortium (2014). Genome-wide trans-ancestry meta-analysis provides insight into the genetic architecture of type 2 diabetes susceptibility. Nat. Genet. *46*, 234–244.
88. Moffatt, M.F., Gut, I.G., Demenais, F., Strachan, D.P., Bouzigon, E., Heath, S., von Mutius, E., Farrall, M., Lathrop, M., Cookson, W.O.; and GABRIEL Consortium (2010). A large-scale, consortium-based genomewide association study of asthma. N. Engl. J. Med. *363*, 1211–1221.
89. N'Diaye, A., Chen, G.K., Palmer, C.D., Ge, B., Tayo, B., Mathias, R.A., Ding, J., Nalls, M.A., Adeyemo, A., Adoue, V., et al. (2011). Identification, replication, and fine-mapping of loci associated with adult height in individuals of african ancestry. PLoS Genet. *7*, e1002298.
90. Gustafsson, A., and Lindenfors, P. (2004). Human size evolution: no evolutionary allometric relationship between male and female stature. J. Hum. Evol. *47*, 253–266.
91. Whiteford, H.A., Degenhardt, L., Rehm, J., Baxter, A.J., Ferrari, A.J., Erskine, H.E., Charlson, F.J., Norman, R.E., Flaxman, A.D., Johns, N., et al. (2013). Global burden of disease attributable to mental and substance use disorders: findings from the Global Burden of Disease Study 2010. Lancet *382*, 1575–1586.
92. de Candia, T.R., Lee, S.H., Yang, J., Browning, B.L., Gejman, P.V., Levinson, D.F., Mowry, B.J., Hewitt, J.K., Goddard, M.E., O'Donovan, M.C., et al.; International Schizophrenia Consortium; and Molecular Genetics of Schizophrenia Collaboration (2013). Additive genetic variation in schizophrenia risk is shared by populations of African and European descent. Am. J. Hum. Genet. *93*, 463–470.
93. Chan, Y., Lim, E.T., Sandholm, N., Wang, S.R., McKnight, A.J., Ripke, S., Daly, M.J., Neale, B.M., Salem, R.M., Hirschhorn, J.N.; DIAGRAM Consortium; GENIE Consortium; GIANT Consortium; IIBDGC Consortium; and PGC Consortium (2014). An excess of risk-increasing low-frequency variants can be a signal of polygenic inheritance in complex diseases. Am. J. Hum. Genet. *94*, 437–452.
94. Minikel, E.V., Vallabh, S.M., Lek, M., Estrada, K., Samocha, K.E., Sathirapongsasuti, J.F., McLean, C.Y., Tung, J.Y., Yu, L.P., Gambetti, P., et al.; Exome Aggregation Consortium (ExAC) (2016). Quantifying prion disease penetrance using large population control cohorts. Sci. Transl. Med. *8*, 322ra9.
95. Li, Y.R., and Keating, B.J. (2014). Trans-ethnic genome-wide association studies: advantages and challenges of mapping in diverse populations. Genome Med. *6*, 91.
96. Rosenberg, N.A., Huang, L., Jewett, E.M., Szpiech, Z.A., Jankovic, I., and Boehnke, M. (2010). Genome-wide association studies in diverse populations. Nat. Rev. Genet. *11*, 356–366.

The American Journal of Human Genetics, Volume *100*

Supplemental Data

Human Demographic History Impacts Genetic Risk Prediction across Diverse Populations

Alicia R. Martin, Christopher R. Gignoux, Raymond K. Walters, Genevieve L. Wojcik, Benjamin M. Neale, Simon Gravel, Mark J. Daly, Carlos D. Bustamante, and Eimear E. Kenny

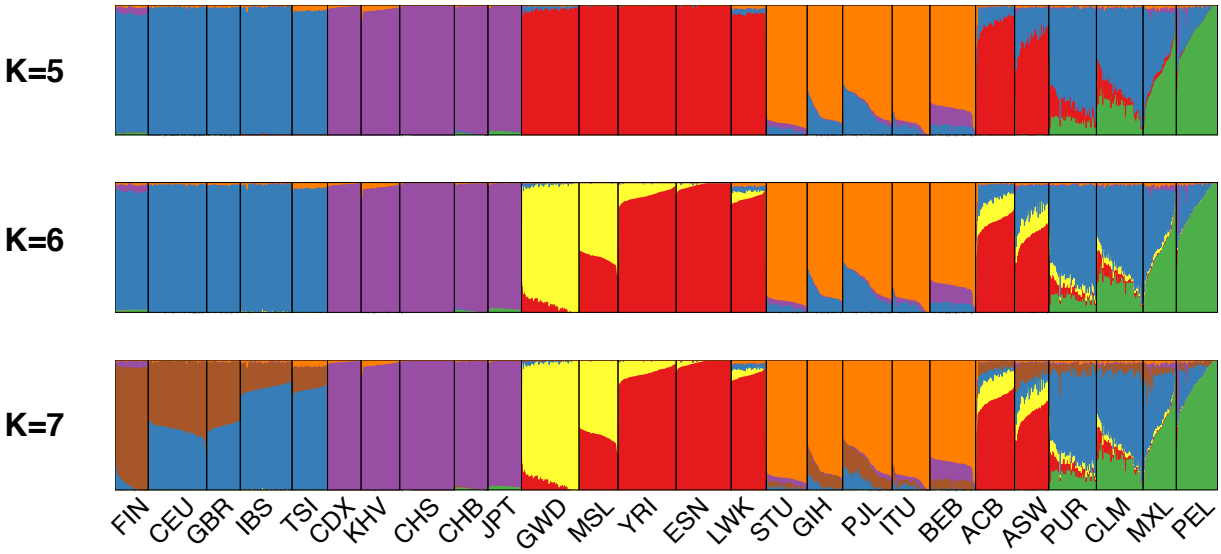

Figure S1 – ADMIXTURE analysis at K=5, K=7, and K=8. K=8 has the lowest 10-fold cross-validation error of K=3-12. At K=5, this analysis separates continental ancestries in the super populations (AFR, AMR, EAS, EUR, and SAS, population abbreviations in Table S1). These results also highlight sub-continental substructure; for example, there is detectable substructure resembling European (EUR) and East Asian (EAS) ancestries in the SAS populations (population means range from 6.1-15.9% and 0.3-12.2%, respectively), with the highest rates of East Asian-like ancestry in the Bengalis from Bangladesh (BEB). In contrast, the greatest quantity of European-like ancestry in the SAS populations is in the Punjabi from Lahore, Pakistan (PJL), who are geographically the closest to Europe. Ancestral clines have been observed along geographical, caste, and linguistic axes in more densely sampled studies of South Asia.[1,2] Increasing the model to K=6 there is also an east-west cline among African populations, while at K=7 we observe the north-south cline of European ancestry.[3] While there is minimal Native American ancestry (<1%) in most African Americans across the United States, there is a substantial enrichment in several ASW individuals from 1000 Genomes (mean of 3.1%, and 9 samples with >5%, including NA19625, NA19921, NA20299, NA20300, NA20314, NA20316, NA20319, NA20414, and NA20274).[4,5] Interestingly, one ASW individual has no African ancestry (NA20314, EUR= 0.40, NAT=0.59) but is the mother of NA20316 in an ASW duo with few Mendelian inconsistencies that suggest that the father mostly likely has ~80% African and ~20% European ancestry, similar to other ASW individuals. We also find evidence of East Asian admixture in several PEL samples (39% in HG01944, 12% in HG02345, 6% in HG0192, 5% in HG01933, and 5% in HG01948). Consistent with the autosomal evidence, the Y chromosome haplogroup for HG01944 (Q1a-M120) clusters most closely with two KHV samples and other East Asians rather than the Q-L54 subgroup expected in samples from South America.[6]

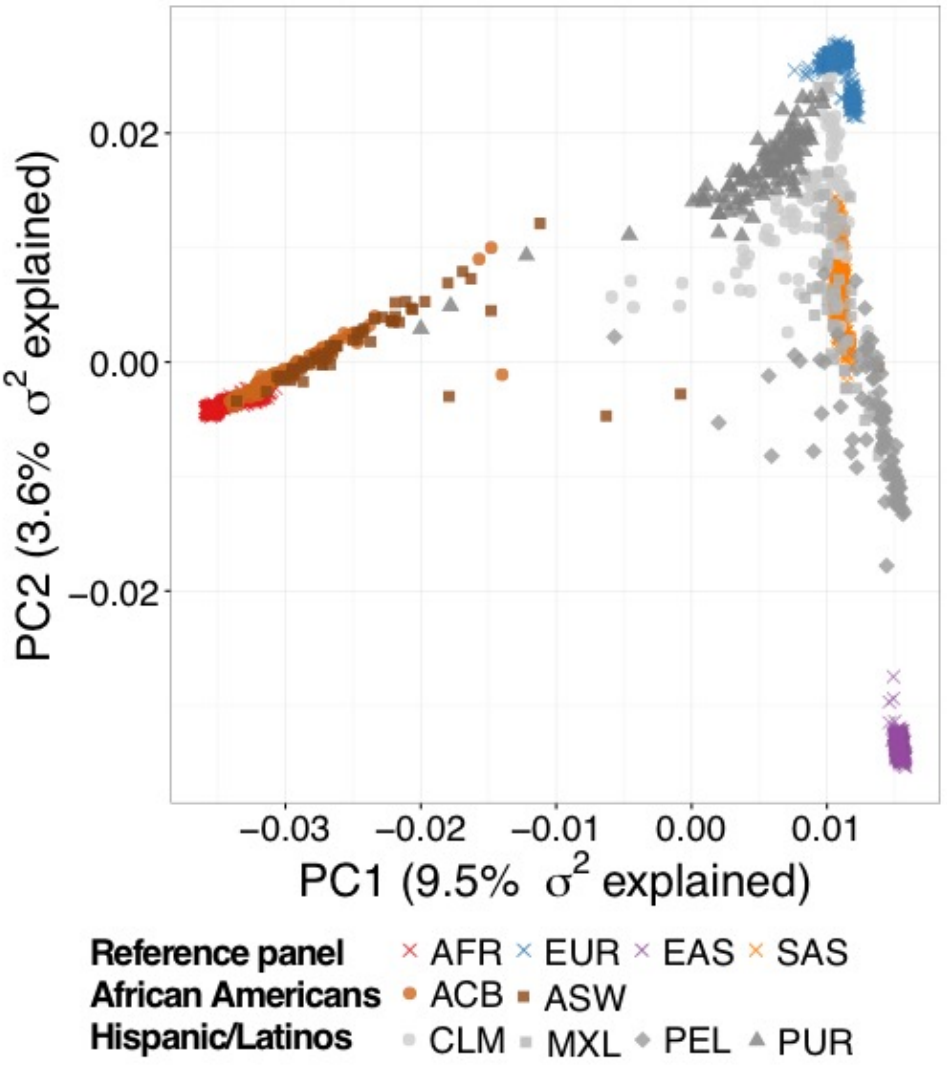

Figure S2 – Principal components analysis of all samples showing the relative homogeneity of AFR, EUR, EAS, and SAS continental groups and continental mixture of admixed samples from the Americas (ACB, ASW, CLM, MXL, PEL, and PUR).

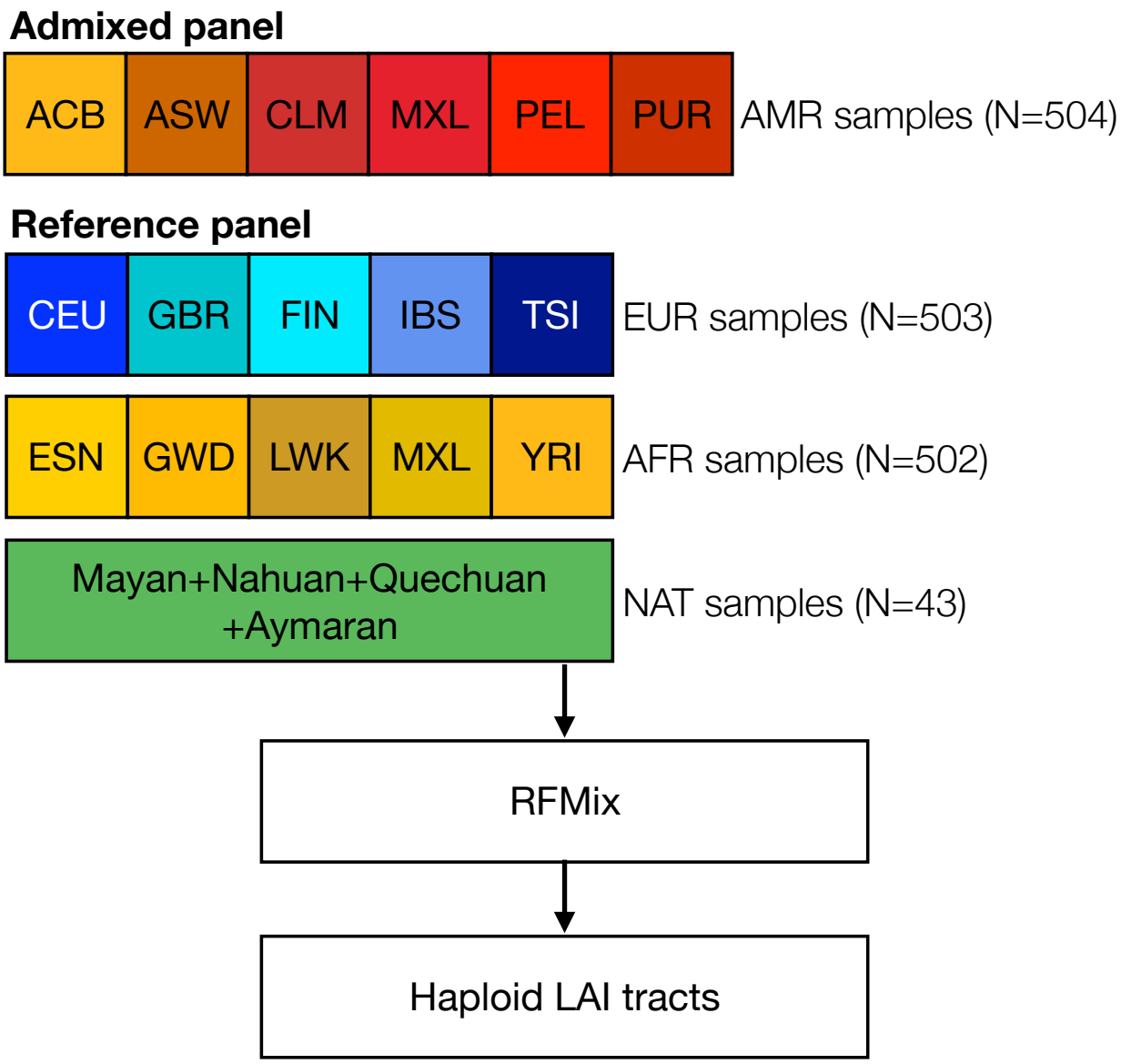

Figure S3 – Schema of local ancestry calling pipeline

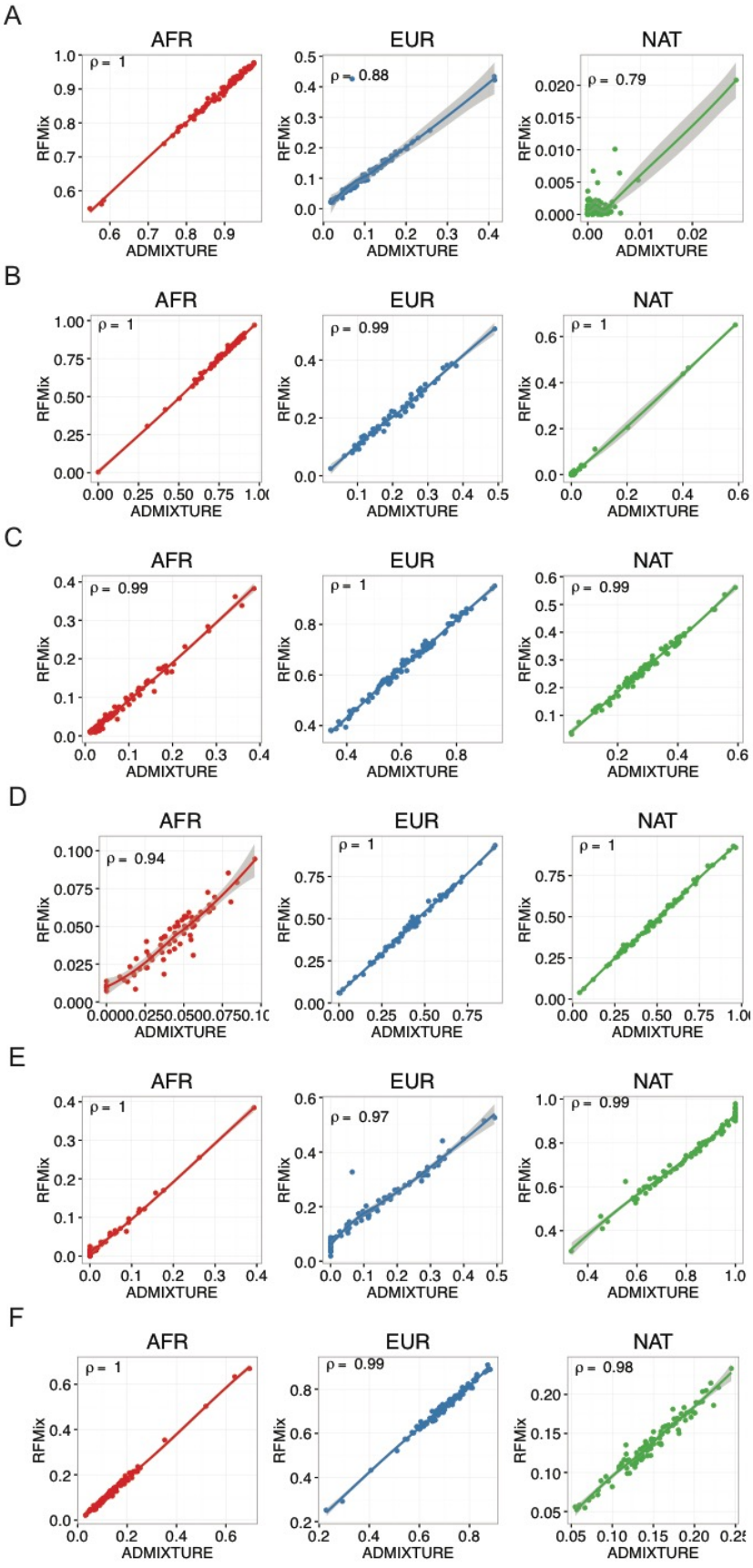
A
AFR
EUR
NAT
ρ = 1
ρ = 0.88
ρ = 0.79
B
ρ = 1
ρ = 0.99
ρ = 1
C
ρ = 0.99
ρ = 1
ρ = 0.99
D
ρ = 0.94
ρ = 1
ρ = 1
E
ρ = 1
ρ = 0.97
ρ = 0.99
F
ρ = 1
ρ = 0.99
ρ = 0.98
RFMix
ADMIXTURE

Figure S4 – Concordance between global ancestry estimates across individuals via Pearson's correlation from ADMIXTURE at K=5 as in Figure S1 versus 3-way RFMix inferences for AFR, EUR, and NAT ancestries. The correlation between ADMIXTURE and global ancestry estimates from RFMix was lower when there was minimal ancestry from a given source population and/or tracts were very short (<5 cM), e.g. NAT ancestry in the ACB (ρ=0.79) and AFR ancestry in the MXL (ρ=0.94). A) ACB. Substantial differences occurred in 1 ACB individual, HG01880, where considerable South Asian ancestry (31.8%) was classified as European ancestry due to limitations of the 3-way local ancestry reference panel. B) ASW. C) CLM. D) MXL. E) PEL. Substantial differences occurred in 2 PEL individuals, HG01944 and HG02345, where considerable East Asian ancestry (38.2% and 12.3%, respectively) was classified in RFMix as EUR and NAT ancestry due to limitations of the 3-way local ancestry reference panel. F) PUR.

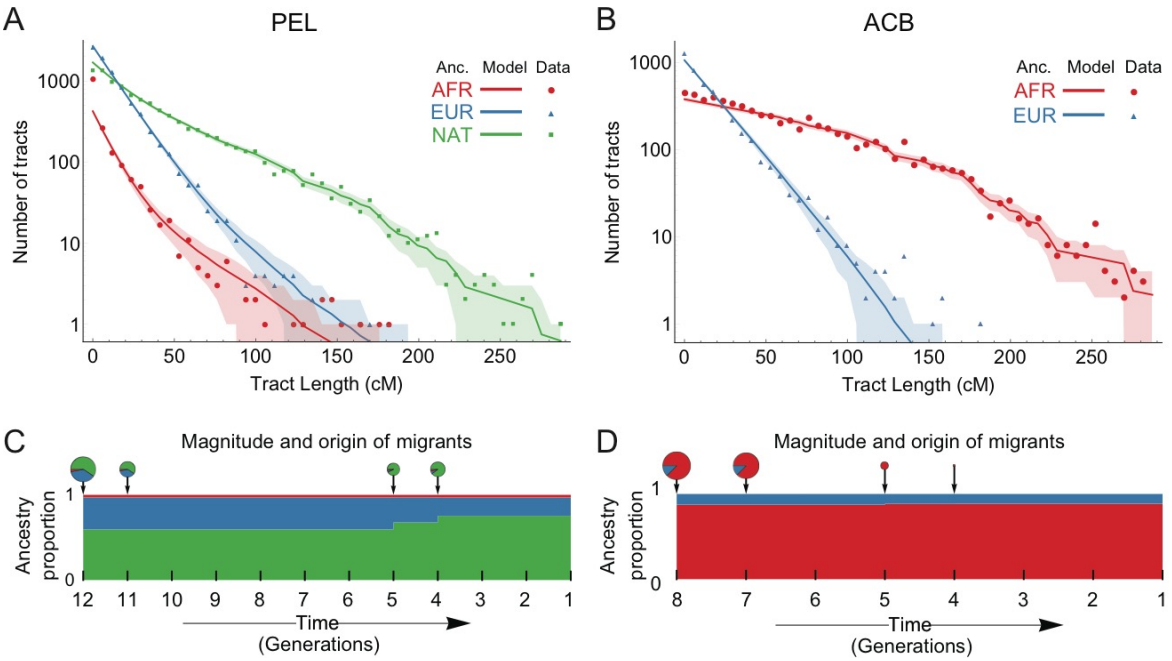

Figure S5 – Demographic reconstruction through genetically dated recent admixture events in the Americas. A-B) Local ancestry tract length decay of AFR, EUR, and NAT continental ancestry tracts for the A) PEL and B) ACB. Points represent the observed distribution of ancestry tracts, and solid lines represent the distribution of the best-fit Markov model inferred using *Tracts*, with the shaded areas indicating one standard deviation confidence intervals. C-D) Admixture time estimates in number of generations ago, relative quantity of migrants, and ancestry proportions over time under the best-fitting model for the C) PEL and D) ACB. C) The best-fit model for the PEL begins ~12 generations ago, which is slightly more recent than for insular and Caribbean mainland populations. For example, admixture in Colombian and Honduran mainland populations was previously inferred to have begun 14 generations ago, whereas admixture in Cuban, Puerto Rican, Dominican, and Haitian populations began 16-17 generations ago.[7] There is minimal African ancestry (2.9%), some European ancestry (37.6%) and primarily Native ancestry (59.4%) in the first pulse of admixture, followed by a later pulse (~5 generations ago) of primarily Native ancestry (91.1%). This later pulse of primarily Native ancestry is unique to the PEL compared to other admixed populations of the Americas.[7] D) The best-fit model for the ACB was an initial pulse of admixture between Europeans and Africans followed by a later pulse of African ancestry. The best model indicates that admixture in the ACB began ~8 generations ago with the initial pulse containing 87.4% African ancestry and 12.6% European ancestry. The second pulse of African ancestry began ~5 generations ago and had only a minor overall contribution (4.4% of total pulse ancestry), which is consistent with either a later small pulse of African ancestry or movement of populations within the Caribbean. The admixture events we infer in the ACB are more recent than previous ASW and African American two-pulse models, which estimated that admixture began ~10-11 generations ago.[4,8] Potential explanations for this small difference include differences in the ages of individual between the two cohorts and the fact that pulse timings indicate the generations that admixture most likely spanned rather than the exact generation during which admixture began.[7]

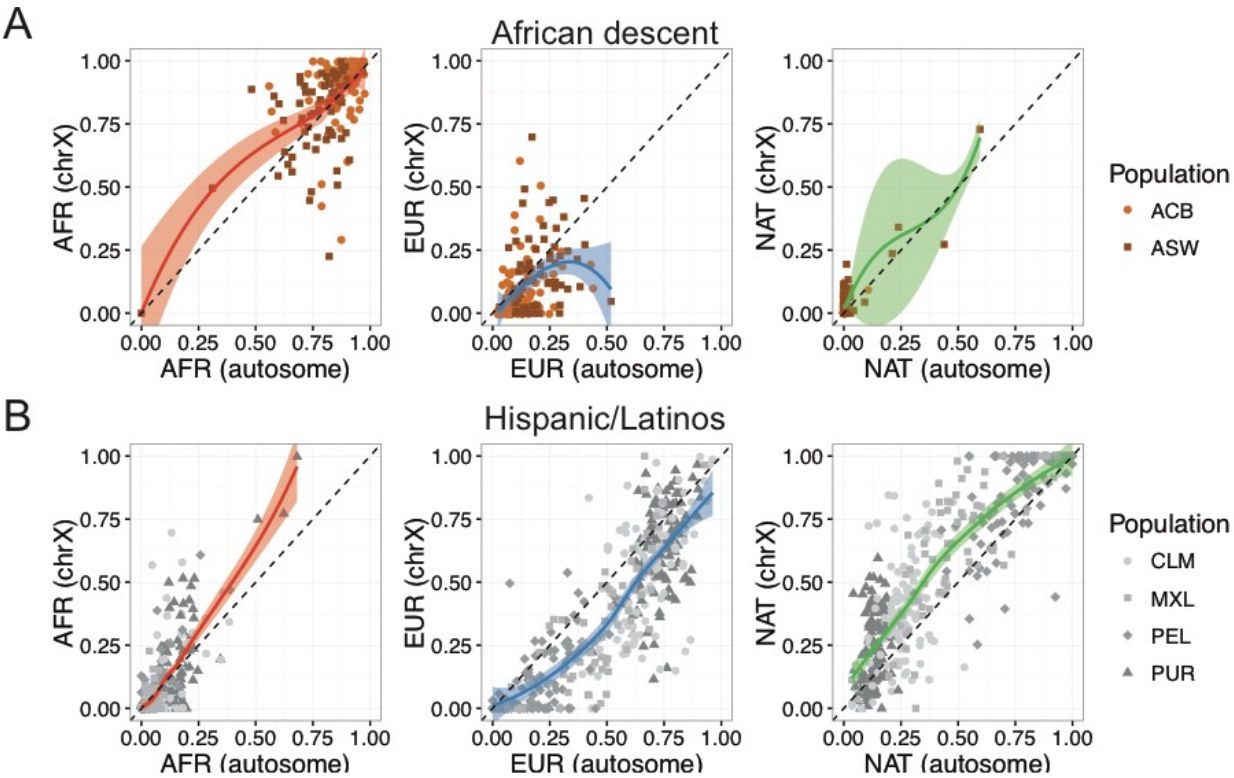

Figure S6 – Comparison of ploidy-adjusted ADMIXTURE ancestry estimates obtained on the autosomes and X chromosome at K=3 with CEU, YRI, and NAT[9] reference samples. 700,093 SNPs on the autosomes and 10,503 SNPs on the X chromosome were used to infer ancestry proportions. A) African descent and B) Hispanic/Latino samples. Sex-biased admixture has previously been shown to be ubiquitous in the Americas, impacting phenotypes strongly correlated with ancestry, such as pigmentation.[7,10-14] We inferred sex-biases in admixture events by separately querying ploidy-adjusted admixture proportions on the X chromosome versus the autosomes, as previously described[10]. We computed 3-way admixture proportions for AMR and AFR/AMR via ADMIXTURE[15] and consistently find across all six admixed AMR populations that the ratio of European ancestry is significantly depleted on the X chromosome compared to the autosomes, indicating a ubiquitous excess of breeding European males in the Americas, as seen previously[4,12,16]; there is also a significant excess of Native American ancestry ($p<1e-2$, Table S3) on the X chromosome in each of the AMR populations ($p < 1e-4$).

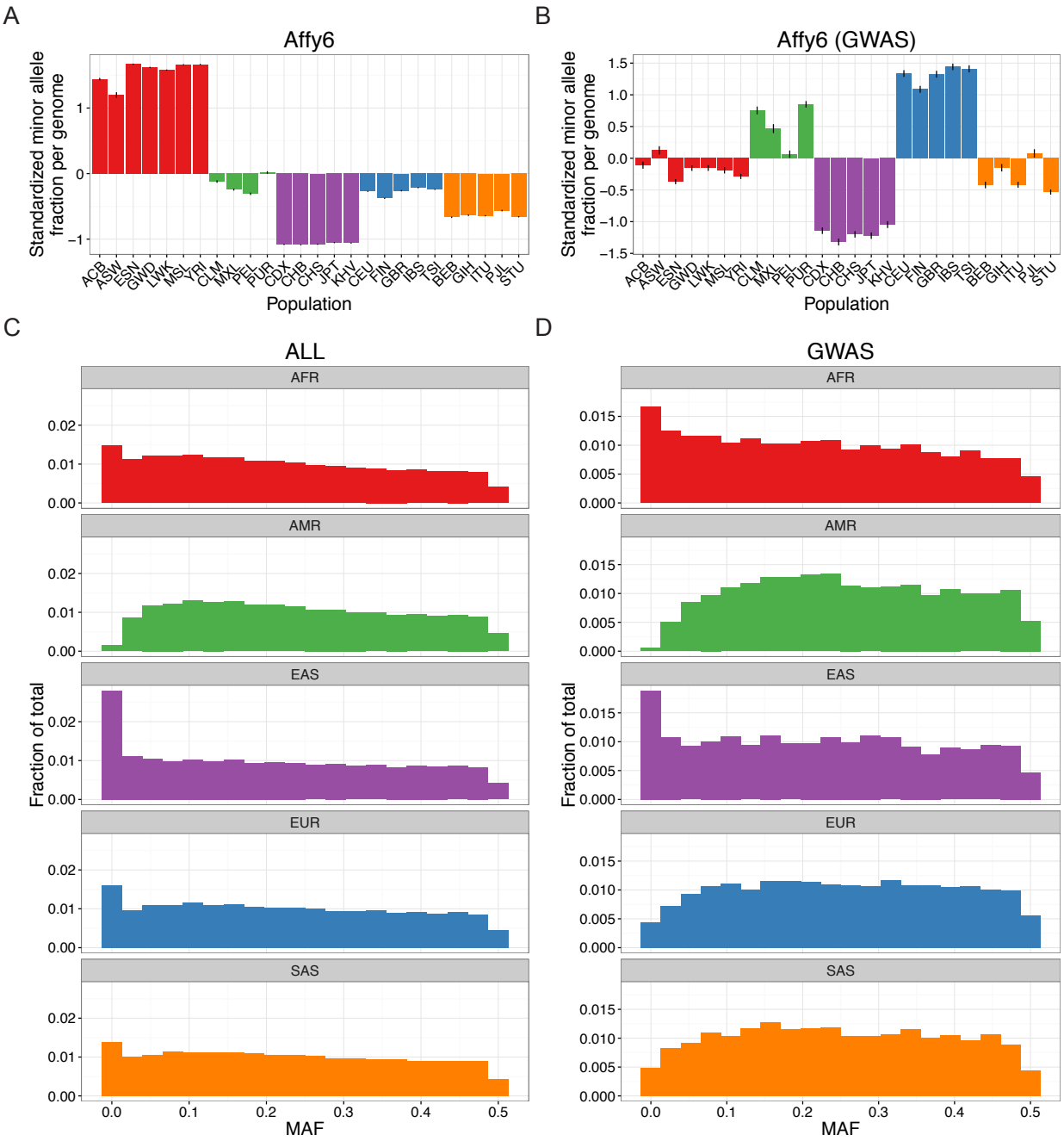

Figure S7 – Genetic variation and allele frequencies in global populations across all sites and at GWAS sites. A-B) GWAS study bias in European and American samples compared at all Affy6 sites from which local ancestry calls were made. All standardizations are computed as the ratio of minor alleles to total alleles per population minus the mean ratio across all individuals, then all divided by the standard deviation of this ratio. Error bars shows the standard error of the mean. A) Standardized across all Affy6 sites. B) Standardized across the intersection of Affy6 sites and the GWAS catalog. C-D) Allele frequencies within all super populations. Minor allele frequency fraction across C) all sites Affy6 sites, and D) the intersection of all Affy6 and GWAS catalog sites.

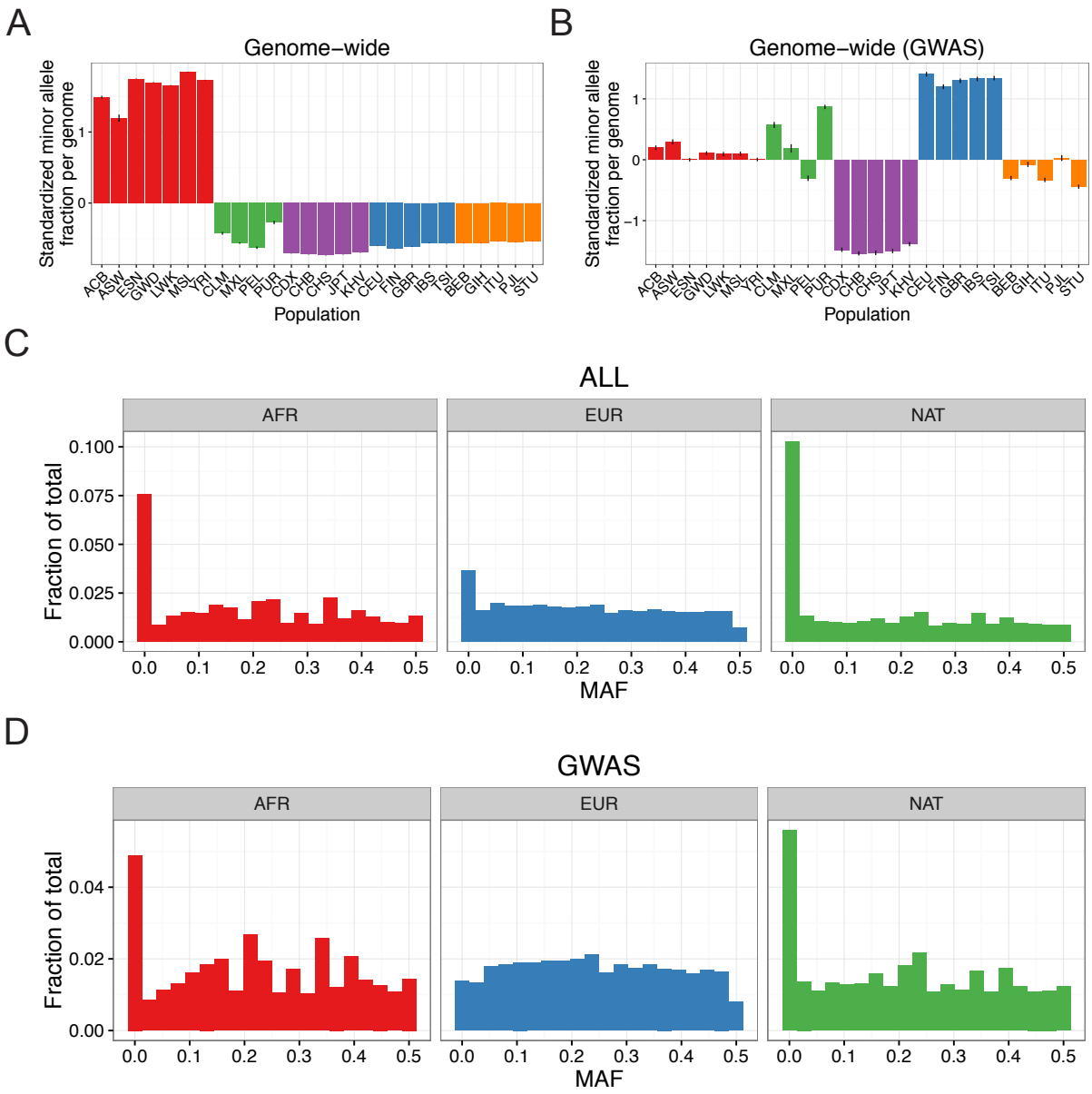

Figure S8 – Genetic variation in global and admixed populations across all sites and at GWAS sites. A-B) GWAS study bias in European and American samples compared to genomic background. All standardizations are computed as the ratio of minor alleles to total alleles per population minus the mean ratio across all individuals from all populations, then all divided by the standard deviation of this ratio. Error bars shows the standard error of the mean. A) Standardized across the whole genome. B) Standardized across all sites from the GWAS catalog. C-D) Allele frequencies in local ancestry calls from admixed AMR and AFR/AMR samples are specifically enriched on European tracts and depleted on African and Native American tracts across all genotyped sites and specifically at GWAS sites. Minor allele frequency fraction across C) all sites in admixed AFR/AMR and AMR populations stratified by local ancestry tracts, and D) sites from the GWAS catalog in admixed AFR/AMR and AMR populations stratified by local ancestry tracts.

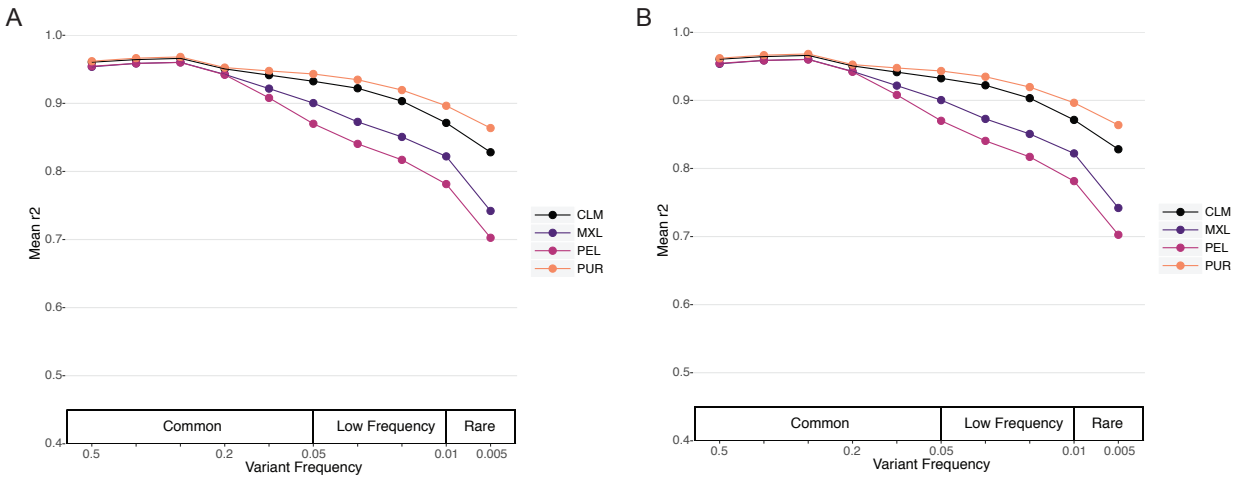

Figure S9 – Imputation accuracy by population for chromosome 9. A) Illumina OmniExpress. B) Affymetrix Axiom World Array LAT

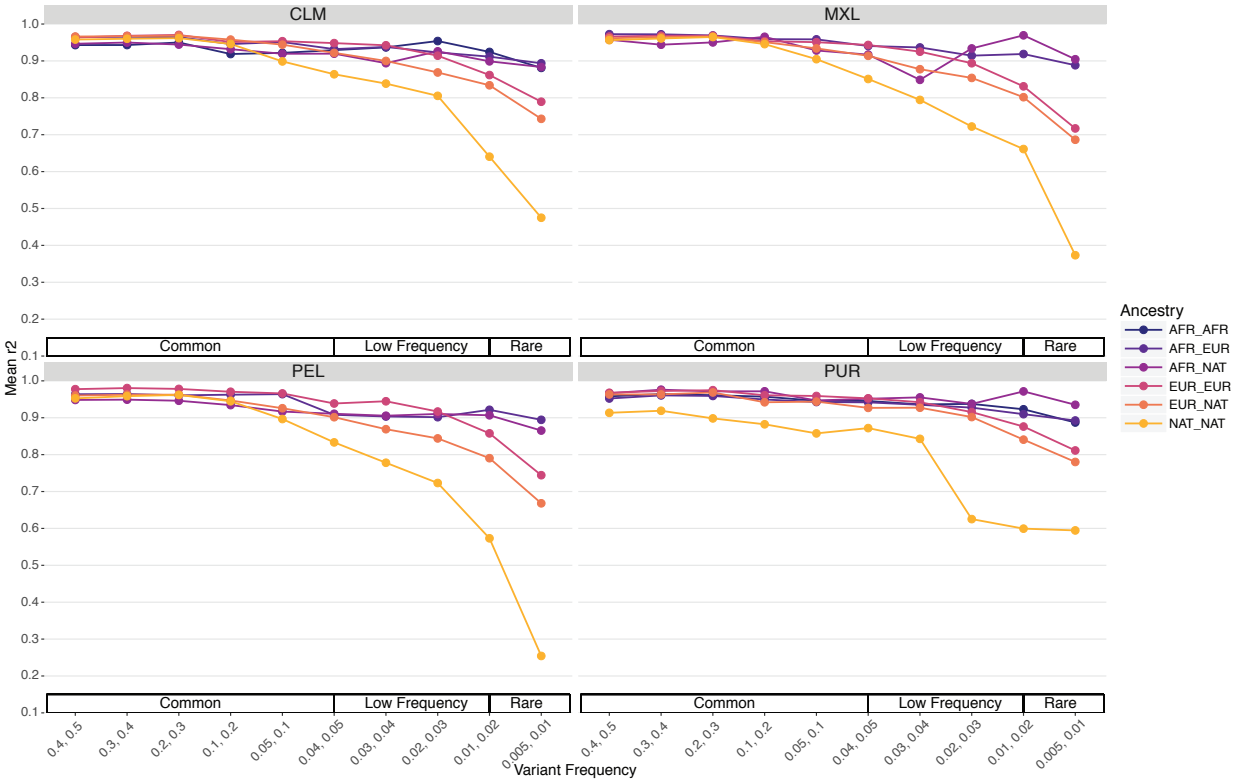

Figure S10 – Imputation accuracy by population assessed using a leave-one-out strategy, stratified by diploid local ancestry on chromosome 9 for the Affymetrix Axiom World Array LAT genotyping array.

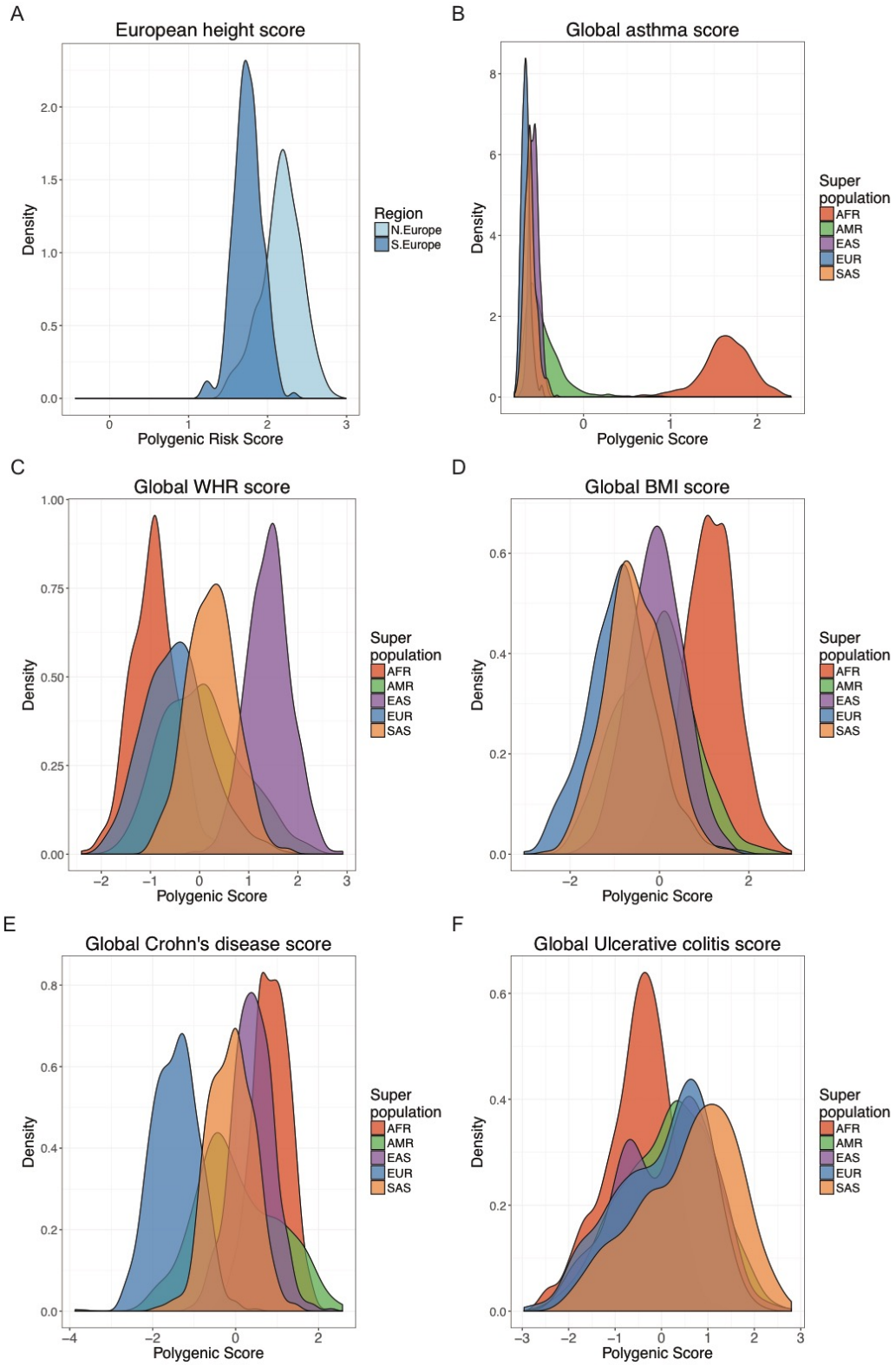

Figure S11 – Standardized polygenic risk score distributions for: A) northern/southern European height, B) asthma, C) waist-hip ratio, D) body mass index, E) Crohn's disease, and F) ulcerative colitis.

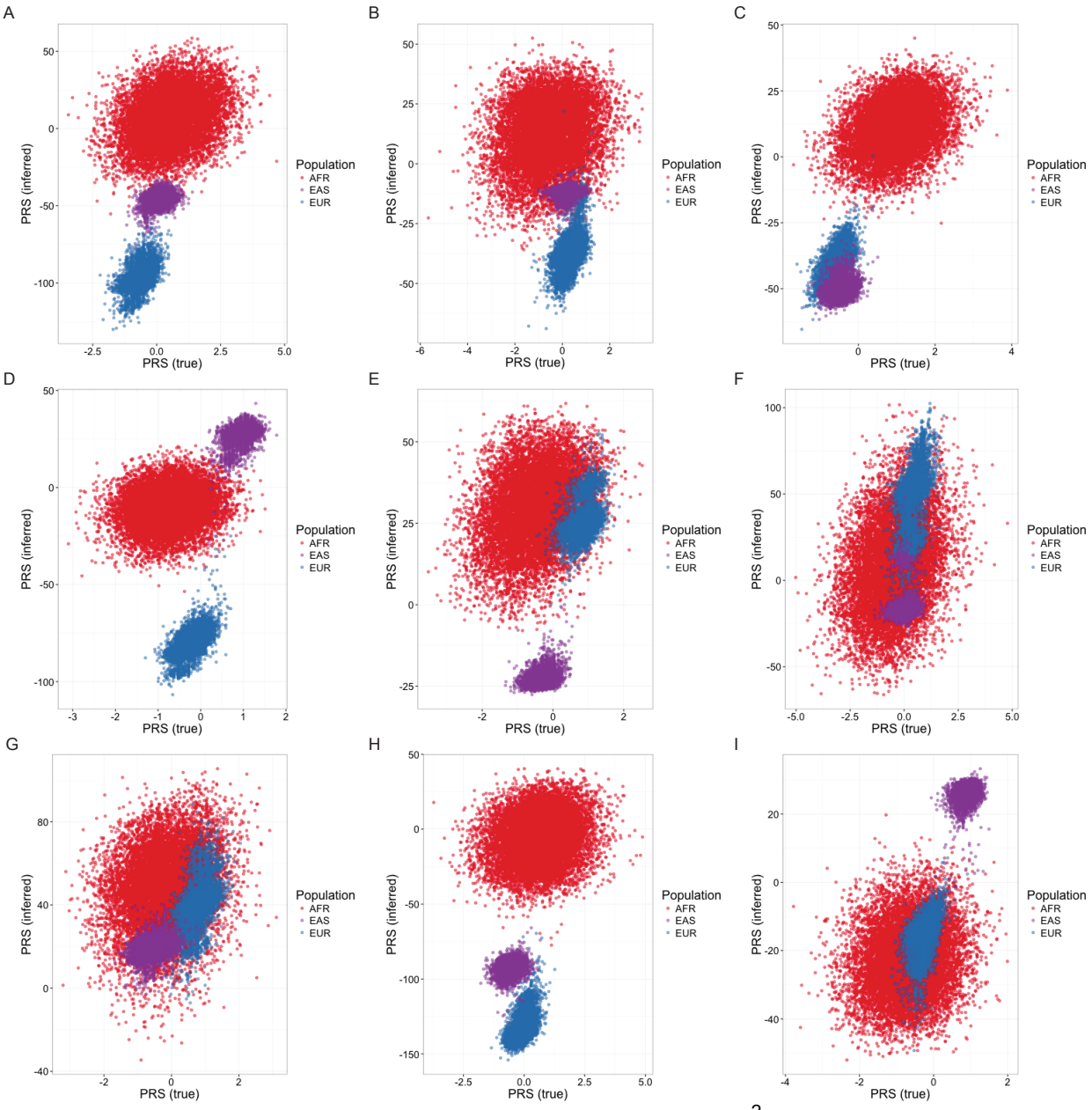

Figure S12 – Simulation runs for the same parameter set (h^2=0.67, m=1000) and same causal variants with varying effect sizes resulting in a wide range of possible biases in inferred polygenic risk scores across populations.

A

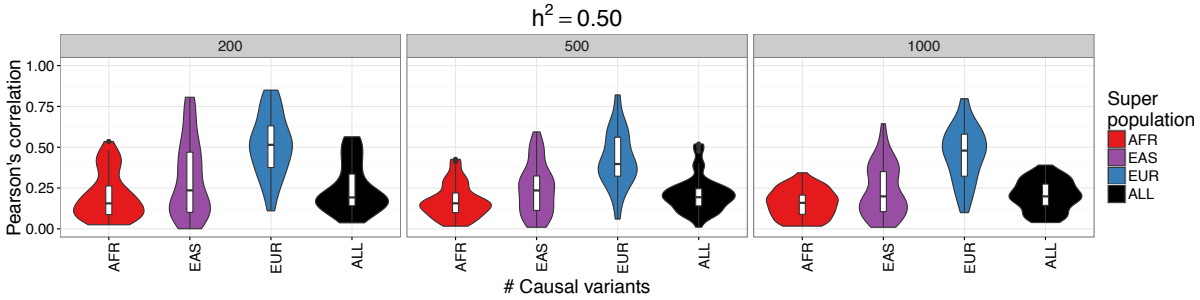

B

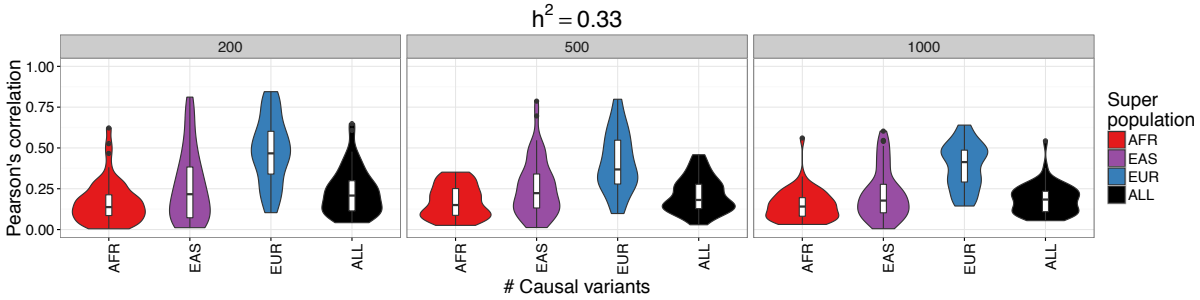

Figure S13 - Violin plots show Pearson's correlation across 50 iterations per parameter set between true and inferred polygenic risk scores across differing genetic architectures, including *m*=200, 500, and 1,000 causal variants and h^2=0.67, as in Figure 5. The "ALL" population correlations were performed on population mean-centered true and inferred polygenic risk scores.

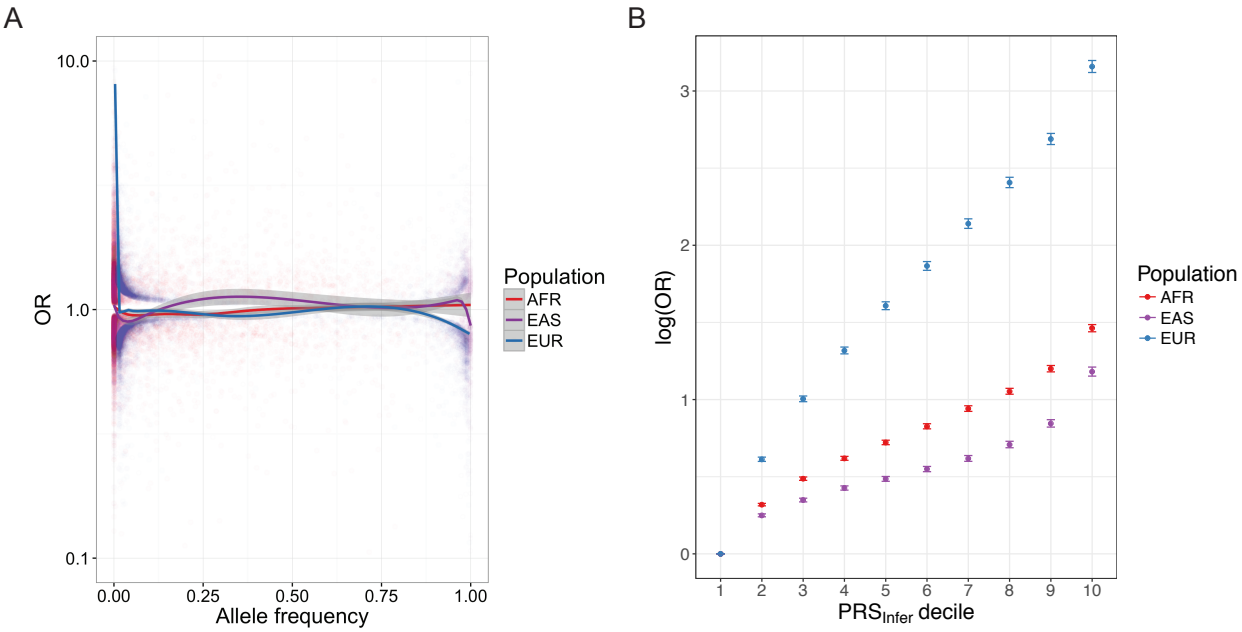

Figure S14 – **Genetic risk prediction differences across populations.** A) Allele frequency versus inferred odds ratio for sites included in inferred polygenic risk scores for each population across 500 simulations, as in Figure 5A-B. B) Log odds ratio by inferred polygenic risk score. The 10,000 individuals with the highest total liability per population were designated as cases, and 10,000 random other individuals in the population were designated as controls. The polygenic risk scores were converted to ordinal deciles, and contrasted with the 1st decile through logistic regression, as: case/control status predicted by polygenic risk decile and population label. Error bars indicate the standard error of the mean across 500 replicates with h^2=0.67 and m=1000 causal variants, as in Figure 5A-B. Small divergence from the population trend of prediction accuracy across the AFR and EAS are driven by differences in population-specific heritabilities arising from different numbers of population-private causal alleles (i.e. more AFR variants in general gives rise to more AFR-specific causal variants).

Table S1 – Population names and abbreviations

Population	Code	Super population	N
Esan in Nigeria	ESN	AFR	99
Gambian in Western Division, Mandinka	GWD	AFR	113
Luhya in Webuye, Kenya	LWK	AFR	99
Mende in Sierra Leone	MSL	AFR	85
Yoruba in Ibadan, Nigeria	YRI	AFR	108
African Caribbean in Barbados	ACB	AFR/AMR	96
People with African Ancestry in Southwest USA	ASW	AFR/AMR	61
Colombians in Medellin, Colombia	CLM	AMR	94
People with Mexican Ancestry in Los Angeles, CA, USA	MXL	AMR	64
Peruvians in Lima, Peru	PEL	AMR	85
Puerto Ricans in Puerto Rico	PUR	AMR	104
Chinese Dai in Xishuangbanna, China	CDX	EAS	93
Han Chinese in Beijing, China	CDX	EAS	103
Southern Han Chinese	CHS	EAS	105
Japanese in Tokyo, Japan	JPT	EAS	104
Kinh in Ho Chi Minh City, Vietnam	KHV	EAS	99
Utah residents (CEPH) with Northern and Western European ancestry	CEU	EUR	99
British in England and Scotland	GBR	EUR	91
Finnish in Finland	FIN	EUR	99
Iberian Populations in Spain	IBS	EUR	107
Toscani in Italia	TSI	EUR	107
Bengali in Bangladesh	BEB	SAS	86
Gujarati Indians in Houston, TX, USA	GIH	SAS	103
Indian Telugu in the UK	ITU	SAS	102
Punjabi in Lahore, Pakistan	PJL	SAS	96
Sri Lankan Tamil in the UK	STU	SAS	102

Table S2 – Three-way admixture proportions between recently admixed populations in the Americas. Values are computed at K=3 on common autosomal SNPs using ADMIXTURE with mean percentages ± standard deviations.

	AFR	EUR	NAT
ACB	88.0% (7.7%)	11.7% (7.3%)	0.3% (1.1%)
ASW	75.6% (13.8%)	21.3% (9.1%)	3.1% (9.2%)
CLM	7.8% (13.8%)	66.6% (12.8%)	25.7% (9.3%)
MXL	4.3% (2.2%)	48.7% (18.6%)	47.0% (19.1%)
PEL	2.5% (5.4%)	20.2% (12.0%)	77.3% (14.2%)
PUR	13.9% (5.4%)	73.2% (10.0%)	12.9% (3.6%)

Table S3 – Comparison of mean ancestry proportions and ratio on chromosome X versus autosomes across populations. Per Lind et al[10], proportion X in a population = (fraction male + 2*fraction female) / 1.5, and proportion autosome in a population = fraction male + fraction female. P-values are from two-sided t-tests on individual ancestries (comparisons are not independent as ancestry proportions must sum to one).

	Ancestry	ACB	ASW	CLM	MXL	PEL	PUR
Relative X/autosome % change	AFR	4.01	0.83	-2.02	-20.32	50.75	12.69
	EUR	-41.73	-17.41	-20.20	-26.60	-41.51	-14.51
	NAT	558.04	87.41	52.70	28.49	9.37	66.89
p-value	AFR	8.9e-2	7.7e-1	9.8e-1	6.8e-2	3.5e-1	4.1e-1
	EUR	1.0e-3	8.9e-2	1.4e-7	7.9e-4	4.5e-6	1.5e-7
	NAT	7.2e-9	1.1e-1	4.0e-9	3.9e-4	1.3e-3	1.4e-10

Table S4 – Empirical polygenic risk score details. OR = odds ratio

Trait	Reference	Effect size	Number of clumps with p≤1e-2
Height	Wood et al, 2014	Beta	35,194
Female WHR	Shungin et al, 2015	Beta	7,351
T2D, EUR	Gaulton et al, 2015	Log(OR)	515
T2D, Multi-ethnic	Mahajan et al, 2014	Log(OR)	11,577
Asthma	Moffatt et al, 2010	Log(OR)	4,786
Schizophrenia	Ripke et al, 2014	Log(OR)	22,047
BMI	Locke et al, 2015	Beta	9,445
Crohn's disease	Jostins et al, 2012	Log(OR)	19,637
Ulcerative colitis	Jostins et al, 2012	Log(OR)	19,078

References

1. Basu A, Sarkar-Roy N, Majumder PP (2016) Genomic reconstruction of the history of extant populations of India reveals five distinct ancestral components and a complex structure. Proc Natl Acad Sci U S A 113:1594-1599
2. Reich D, Thangaraj K, Patterson N, Price AL, Singh L (2009) Reconstructing Indian population history. Nature 461:489-494
3. Novembre J, Johnson T, Bryc K, Kutalik Z, Boyko AR, Auton A, et al (2008) Genes mirror geography within Europe. Nature 456:98-101
4. Baharian S, Barakatt M, Gignoux CR, Shringarpure S, Errington J, Blot WJ, et al (2016) The Great Migration and African-American Genomic Diversity. PLoS genetics 12:e1006059
5. Mimno D, Blei DM, Engelhardt BE (2015) Posterior predictive checks to quantify lack-of-fit in admixture models of latent population structure. Proc Natl Acad Sci U S A 112:E3441-E3450
6. Poznik GD, Xue Y, Mendez FL, Willems TF, Massaia A, Wilson Sayres MA, et al (2016) Punctuated bursts in human male demography inferred from 1,244 worldwide Y-chromosome sequences. Nature Genetics
7. Moreno-Estrada A, Gravel S, Zakharia F, McCauley JL, Byrnes JK, Gignoux CR, et al (2013) Reconstructing the Population Genetic History of the Caribbean. PLoS Genetics 9:e1003925
8. Gravel S (2012) Population genetics models of local ancestry. Genetics 191:607-619
9. Mao X, Bigham AW, Mei R, Gutierrez G, Weiss KM, Brutsaert TD, et al (2007) A genomewide admixture mapping panel for Hispanic/Latino populations. American journal of human genetics 80:1171-1178
10. Lind JM, Hutcheson-Dilks HB, Williams SM, Moore JH, Essex M, Ruiz-Pesini E, et al (2007) Elevated male European and female African contributions to the genomes of African American individuals. Human Genetics 120:713-722
11. Bryc K, Auton A, Nelson MR, Oksenberg JR, Hauser SL, Williams S, et al (2010) Genome-wide patterns of population structure and admixture in West Africans and African Americans. Proceedings of the National Academy of Sciences of the United States of America 107:786-791
12. Bryc K, Durand EY, Macpherson JM, Reich D, Mountain JL (2015) The genetic ancestry of African Americans, Latinos, and European Americans across the United States. American Journal of Human Genetics 96:37-53
13. Beleza S, Campos J, Lopes J, Araújo II, Hoppfer Almada A, Correia e Silva A, et al (2012) The Admixture Structure and Genetic Variation of the Archipelago of Cape Verde and Its Implications for Admixture Mapping Studies. PLoS ONE 7:1-12
14. Marcheco-Teruel B, Parra EJ, Fuentes-Smith E, Salas A, Buttenschøn HN, Demontis D, et al (2014) Cuba: exploring the history of admixture and the genetic basis of pigmentation using autosomal and uniparental markers. PLoS genetics 10:e1004488
15. Shringarpure SS, Bustamante CD, Lange KL, Alexander DH (2016) Efficient analysis of large datasets and sex bias with ADMIXTURE. BMC Bioinformatics 17(1):218
16. McHugh C, Thornton TA, Brown L (2015) Detecting Heterogeneity in Population Structure Across the Genome in Admixed Populations. Genetics 204(1):43-56